

APPLICATION OF
STEEL FIBER REINFORCED CONCRETE
IN SEISMIC BEAM-COLUMN JOINTS

A Thesis
Presented to the
Faculty of
San Diego State University

In Partial Fulfillment
of the Requirements for the Degree
Master of Science
in
Civil Engineering

by
Michael Gebman

THE UNDERSIGNED FACULTY COMMITTEE APPROVES

THE THESIS OF MICHAEL GEBMAN:

Dr. Ziad Bayasi, Chair
Department of Civil and Environmental Engineering

Date

Dr. Fang H. Chou
Department of Civil and Environmental Engineering

Dr. James Burns
Department of Mechanical Engineering

SAN DIEGO STATE UNIVERSITY

Spring 2001

DEDICATION

This thesis is dedicated to my parents, to my brother and to my sister. Their encouragement and support is greatly appreciated.

ACKNOWLEDGMENTS

This research was started in the spring of 1999 by two graduate students at San Diego State University: Jesse Sandoval and Chris Hector under the guidance of Dr. Ziad Bayasi. Chris coordinated the donation of the steel bars for this research, and assisted Jesse with the placement and securing of the steel bars. Jesse was a vital team member who stayed with the research effort until the very end. All of his work is greatly appreciated. My participation started during the Spring Semester of 2000, just before placement of the steel-bar arrangement was completed. I shortly thereafter assumed responsibilities for this research effort to its current completion.

Graduate student Henry Hill joined the project during the summer of 2000 and proved to be of great value from the first day he set foot in the lab. His construction experience was very useful in assisting with the construction of formwork. In addition, his previous work experience as an engineer and special inspector proved to be of great value on the day of concrete placement when several quality tests of the concrete mix had to be conducted. He is thanked for setting up a web site for the research effort.

Dr Bayasi's guidance with the larger research effort and this thesis are greatly appreciated. Dr Chou and Dr Burns are thanked for having served on this thesis review committee.

This project could not have been made possible without the support of many businesses. Superior Ready Mix is appreciated for providing the concrete, Bekaert Corporation for providing the steel fibers and Quality Reinforcing Inc. for donating the steel bars. Other contributors to be thanked include the Concrete Materials Research Institute

(CMRI) at SDSU, Composite Optics Inc., Precision Welding, Measurements Group Inc., A1 Hydraulics, and White Cap Industries. The College of Engineering and the Department of Civil & Environmental Engineering are also appreciated for providing the necessary laboratory space and the assistance of lab technicians Bayard Rehkopf (Department of Civil & Environmental Engineering) and Matt Anderson (Department of Mechanical Engineering).

TABLE OF CONTENTS

	PAGE
ACKNOWLEDGMENTS.....	iv
LIST OF TABLES	x
LIST OF FIGURES.....	xi
CHAPTER	
1. INTRODUCTION.....	1
1.1 Background	1
1.1.1 Reinforced Concrete.....	2
1.1.2 Fiber Reinforced Concrete	2
1.1.2.1 Toughness	5
1.1.2.2 Fiber Mechanisms	6
1.1.2.3 Bridging Action.....	6
1.1.2.4 Workability	7
1.1.2.5 Bond Improvement.....	7
1.2 Problem Statement	8
1.3 Purpose of the Research.....	8
1.4 Organization of the Research.....	8
1.5 Limitations of the Research	9
2. LITERATURE REVIEW.....	10
2.1 Benefits of Steel Fibers.....	10
2.1.1 Ductility and Tensile Toughness.....	10
2.1.2 Damage Tolerance against Multiple Load Cycles	14

CHAPTER	PAGE
2. (continued)	
2.2 Mechanisms	15
2.2.1 Shear Resistance.....	15
2.2.2 Dowel Action	18
2.2.3 Bar Confinement	19
3. EXPERIMENTAL PROGRAM	20
3.1 Objectives	20
3.2 Plan.....	20
3.2.1 Test Fixture	20
3.2.2 Load Pattern and Application.....	24
3.3 Joint Design.....	26
3.3.1 Conventional Joint Design.....	26
3.3.2 Half-Scale Joint Design.....	26
3.4 Test Setup.....	29
3.4.1 Strain Gage Locations	29
3.4.2 Setup of Equipment.....	30
3.5 Construction	32
3.5.1 Loading Plates.....	32
3.5.2 Placement of Concrete	36
3.6 Quality Control	37
3.6.1 Fresh Concrete	37
3.6.2 Hardened Concrete	38
3.7 Materials	38
3.7.1 Plain Concrete	38

CHAPTER	PAGE
3. (continued)	
3.7.2 Steel Fibers	39
3.7.3 Steel Reinforcing Bars	39
3.7.4 Anchor Bolts	39
3.7.5 Strain Gages	40
4. RESULTS	42
4.1 Hysteresis Loops	42
4.2 Strain Plots	49
4.3 Quality Testing Results	67
4.3.1 Compression Tests	67
4.3.2 Bending Tests	67
4.3.3 Other Tests	67
5. ANALYSIS	68
5.1 Hysteresis Loop Envelop	68
5.2 Energy Absorption Capacity of Each Loop	68
5.3 Durability	71
5.3.1 Beam Cracking	71
5.3.2 Column Cracking	72
5.3.3 Joint Cracking	72
5.4 Seismic Resistance	78
5.5 Strains	78
6. CONCLUSION	86
6.1 Comparisons with Previous Studies	86
6.2 Seismic Strength	87

CHAPTER	PAGE
6. (continued)	
6.3 Simplification of Construction.....	87
6.4 Design Recommendations.....	88
REFERENCES	89
APPENDICES	
A. STRAIN DATA FOR BEAM-COLUMN JOINTS	92
B. LOAD CELL STRAIN DATA FOR BEAM-COLUMN JOINTS.....	126
C. BEAM-COLUMN JOINT STRAIN DATA PLOTS	160
D. LOAD CELL STRAIN PLOTS	188
E. PHOTOGRAPHIC TESTING HISTORY	195
F. 1997 UNIFORM BUILDING CODE PERTAINING TO BEAM-COLUMN JOINT DESIGN	241
ABSTRACT	246

LIST OF TABLES

TABLE	PAGE
5.1	Energy Absorbed During the Simulated Quasi-static Earthquake Loading.....70
5.2	Maximum Loads Reached During the Simulated Quasi-static Earthquake Loading.....78
A.1	Strain Data for Beam-Column Joint #193
A.2	Strain Data for Beam-Column Joint #297
A.3	Strain Data for Beam-Column Joint #3105
A.4	Strain Data for Beam-Column Joint #4115
A.5	Strain Data for Beam-Column Joint #5118
A.6	Strain Data for Beam-Column Joint #6122
B.1	Load Cell Strain Data for Beam-Column Joint #1127
B.2	Load Cell Strain Data for Beam-Column Joint #2131
B.3	Load Cell Strain Data for Beam-Column Joint #3139
B.4	Load Cell Strain Data for Beam-Column Joint #4149
B.5	Load Cell Strain Data for Beam-Column Joint #5152
B.6	Load Cell Strain Data for Beam-Column Joint #6156

LIST OF FIGURES

FIGURE	PAGE
1.1 Shapes of Steel Fibers	3
1.2 Properties of SFRC.....	4
1.3 Improvements in Joint Behavior Resulting from SFRC.....	5
1.4 Bridging Action of Steel Fibers	7
3.1 Laboratory Setup	21
3.2 Laboratory Layout of Test Specimens.....	22
3.3 View of Specimens Constructed on Top of Each I-Beam.....	23
3.4 Definition of the Elements Comprising a Test Specimen for a Beam-Column Joint	23
3.5 Simulated Quasi-static Earthquake Loading	24
3.6 Beam Displacement During Simulated Earthquake	25
3.7 Setup of Load Cell and Hydraulic Jack.....	25
3.8 Bar Arrangement for a Full-scale Beam-Column Joint.....	27
3.9 Bar Arrangement for a Typical Test Specimen.....	28
3.10 Bar Arrangement under Construction for a Plain Concrete Test Specimen.....	29
3.11 Location of Strain Gages on a Typical Test Beam-Column Joint	30
3.12 Test Specimen Ready for Loading	31
3.13 Data Acquisition System, PC, and Test Setup.....	31
3.14 Alignment of Loading Plates, Hydraulic Jack and Load Cell.....	33
3.15 Typical Test Specimen Ready for Beam-Column Testing.....	34
3.16 Detail of J-bolt Placement in a Typical Beam.....	34
3.17 Detail of Strong Wall	35
3.18 Detail of Base Plate Embedded within Strong Wall	35
3.19 Internal Vibration of SFRC	36
3.20 Test Specimens shortly after Concrete Placement	37
3.21 SFRC	38
3.22 Protected Strain Gages	41

FIGURE	PAGE
4.1 Hysteresis Loop for SFRC Beam-Column Joint #1 with 6-in (15.2-cm) Spacing	43
4.2 Hysteresis Loop for SFRC Beam-Column Joint #5 with 6-in (15.2-cm) Spacing	44
4.3 Hysteresis Loop for SFRC Beam-Column Joint #2 with 8-in (20.3-cm) Spacing	45
4.4 Hysteresis Loop for SFRC Beam-Column Joint #4 with 8-in (20.3-cm) Spacing	46
4.5 Hysteresis Loop for Plain Beam-Column Joint #3 with 4-in (10.2-cm) Spacing	47
4.6 Hysteresis Loop for Plain Beam-Column Joint #6 with 4-in (10.2-cm) Spacing	48
4.7 BC-Joint # 1 History of Strain vs. Normalized Displacement for #5 Bar within Beam.....	50
4.8 BC-Joint #1 History of Strain vs. Normalized Displacement for #4 Bar within Beam.....	51
4.9 BC-Joint #1 History of Strain vs. Normalized Displacement for top Column Bar	52
4.10 BC-Joint #5 History of Strain vs. Normalized Displacement for #5 Bar within Beam.....	53
4.11 BC-Joint #5 History of Strain vs. Normalized Displacement for #4 Bar within Beam.....	54
4.12 BC-Joint #2 History of Strain vs. Normalized Displacement for #5 Bar within Beam.....	55
4.13 BC-Joint #2 History of Strain vs. Normalized Displacement for #4 Bar within Beam.....	56
4.14 BC-Joint #2 History of Strain vs. Normalized Displacement for Top Column Bar	57
4.15 BC-Joint #2 History of Strain vs. Normalized Displacement for Bottom Column Bar	58
4.16 BC-Joint #4 History of Strain vs. Normalized Displacement for #4 Bar within Beam.....	59
4.17 BC-Joint #4 History of Strain vs. Normalized Displacement for Bottom Column Bar	60
4.18 BC-Joint #3 History of Strain vs. Normalized Displacement for #5 Bar within Beam.....	61

FIGURE	PAGE
4.19 BC-Joint #3 History of Strain vs. Normalized Displacement for #4 Bar within Beam.....	62
4.20 BC-Joint #3 History of Strain vs. Normalized Displacement for Bottom Column Bar	63
4.21 BC-Joint #6 History of Strain vs. Normalized Displacement for #5 Bar within Beam.....	64
4.22 BC-Joint #6 History of Strain vs. Normalized Displacement for #4 Bar within Beam.....	65
4.23 BC-Joint #6 History of Strain vs. Normalized Displacement for Top Column Bar	66
5.1 Hysteresis Envelop Curves.....	69
5.2 Observed Damage Patterns.....	71
5.3 Observations after Cycle 2	74
5.4 Observations after Cycle 3	75
5.5 Observations after Cycle 4	76
5.6 Observations after Cycle 5	77
5.7 Strain Comparison between Joints 1 and 3 for #5 Beam Bar.....	80
5.8 Strain Comparison between Joints 1 and 3 for #4 Beam Bar.....	81
5.9 Strain Comparison between Joints 1 and 3 for Top Column Bar.....	82
5.10 Strain Comparison between Joints 2 and 6 for #5 Beam Bar.....	83
5.11 Strain Comparison between Joints 2 and 6 for #4 Beam Bar.....	84
5.12 Strain Comparison between Joints 2 and 6 for Top Column Bar.....	85
C.1 Joint #1 Upper Beam Bar Strain Data	161
C.2 Joint #2 Upper Beam Bar Strain Data	162
C.3 Joint #3 Upper Beam Bar Strain Data	163
C.4 Joint #6 Upper Beam Bar Strain Data	164
C.5 Joint #2 Lower Beam Bar Strain Data.....	165
C.6 Joint #3 Lower Beam Bar Strain Data.....	166
C.7 Joint #4 Lower Beam Bar Strain Data.....	167
C.8 Joint #1 Data from Strain Gage 1	168
C.9 Joint #1 Data from Strain Gage 4.....	169
C.10 Joint #1 Data from Strain Gage 2.....	170

FIGURE	PAGE
C.11 Joint #1 Data from Strain Gage 3	171
C.12 Joint #2 Data from Strain Gage 1	172
C.13 Joint #2 Data from Strain Gage 4	173
C.14 Joint #2 Data from Strain Gage 2	174
C.15 Joint #2 Data from Strain Gage 3	175
C.16 Joint #3 Data from Strain Gage 1	176
C.17 Joint #3 Data from Strain Gage 4	177
C.18 Joint #3 Data from Strain Gage 2	178
C.19 Joint #3 Data from Strain Gage 3	179
C.20 Joint #4 Data from Strain Gage 1	180
C.21 Joint #4 Data from Strain Gage 4	181
C.22 Joint #5 Data from Strain Gage 1	182
C.23 Joint #5 Data from Strain Gage 4	183
C.24 Joint #5 Data from Strain Gage 3	184
C.25 Joint #6 Data from Strain Gage 1	185
C.26 Joint #6 Data from Strain Gage 4	186
C.27 Joint #6 Data from Strain Gage 3	187
D.1 Joint #1 Load Cell Strain Data	189
D.2 Joint #2 Load Cell Strain Data	190
D.3 Joint #3 Load Cell Strain Data	191
D.4 Joint #4 Load Cell Strain Data	192
D.5 Joint #5 Load Cell Strain Data	193
D.6 Joint #6 Load Cell Strain Data	194
E.1 Joint #1 After 2nd Cycle.....	196
E.2 Joint #1 After First Half of 3rd Cycle	197
E.3 Joint #1 After 3rd Cycle	198
E.4 Joint #1 After First Half of 4th Cycle.....	199
E.5 Joint #1 After 4th Cycle	200
E.6 Joint #1 After First Half of 5th Cycle.....	201
E.7 Joint #1 After 5th Cycle	202

FIGURE	PAGE
E.8 Joint #2 After 1st Cycle.....	203
E.9 Joint #2 After First Half of 3rd Cycle	204
E.10 Joint #2 After 3rd Cycle	205
E.11 Joint #2 After First Half of 4th Cycle.....	206
E.12 Joint #2 After 4th Cycle	207
E.13 Joint #2 After First Half of 5th Cycle.....	208
E.14 Joint #2 After 5th Cycle	209
E.15 Joint #2 After First Half of 6th Cycle.....	210
E.16 Joint #2 After 6th Cycle	211
E.17 Joint #3 After First Half of 1st Cycle.....	212
E.18 Joint #3 After 1st Cycle.....	213
E.19 Joint #3 After First Half of 2nd Cycle.....	214
E.20 Joint #3 After 2nd Cycle.....	215
E.21 Joint #3 After First Half of 3rd Cycle	216
E.22 Joint #3 After 3rd Cycle	217
E.23 Joint #3 After First Half of 4th Cycle.....	218
E.24 Joint #3 After 4th Cycle	219
E.25 Joint #3 After First Half of 5th Cycle.....	220
E.26 Joint #3 After 5th Cycle	221
E.27 Joint #3 After First Half of 6th Cycle.....	222
E.28 Joint #4 After 1st Cycle.....	223
E.29 Joint #4 After 2nd Cycle.....	224
E.30 Joint #4 After 3rd Cycle	225
E.31 Joint #4 After 4th Cycle	226
E.32 Joint #4 After 5th Cycle	227
E.33 Joint #5 After 2nd Cycle.....	228
E.34 Joint #5 After 3rd Cycle	229
E.35 Joint #5 After 4th Cycle	230
E.36 Joint #5 After 5th Cycle	231
E.37 Joint #6 After 1st Cycle.....	232

FIGURE	PAGE
E.38 Joint #6 After First Half of 2nd Cycle.....	233
E.39 Joint #6 After 2nd Cycle.....	234
E.40 Joint #6 After First Half of 3rd Cycle	235
E.41 Joint #6 After 3rd Cycle	236
E.42 Joint #6 After First Half of 4th Cycle.....	237
E.43 Joint #6 After 4th Cycle	238
E.44 Joint #6 After First Half of 5th Cycle.....	239
E.45 Joint #6 After 5th Cycle	240

CHAPTER 1

INTRODUCTION

Steel Fiber Reinforced Concrete (SFRC) has an untapped potential application in building frames due to its high seismic energy absorption capability and relatively simple construction technique. To tap such potential, the existing body of knowledge on SFRC must be expanded to provide a proper basis for officials to add this method of construction to the provisions of the building code. This thesis aims to add to that body of knowledge through experimental investigation and analysis.

1.1 Background

Concrete is one of the most versatile building materials. It can be cast to fit any structural shape from a cylindrical water storage tank to a rectangular beam or column in a high-rise building. It is readily available in urban areas at relatively low cost. Concrete is strong under compression yet weak under tension. As such, a form of reinforcement is needed. The most common type of concrete reinforcement is via steel bars.

The advantages to using concrete include high compressive strength, good fire resistance, high water resistance, low maintenance, and long service life. The disadvantages to using concrete include poor tensile strength, and formwork requirement. Other disadvantages include relatively low strength per unit weight [1].

1.1.1 Reinforced Concrete

Tensile strength of concrete is typically 8% to 15% of its compressive strength [1]. This weakness has been dealt with over many decades by using a system of reinforcing bars (rebars) to create reinforced concrete; so that concrete primarily resists compressive stresses and rebars resist tensile and shear stresses.

The longitudinal rebar in a beam resists flexural (tensile stress) whereas the stirrups, wrapped around the longitudinal bar, resist shear stresses. In a column, vertical bars resist compression and buckling stresses while ties resist shear and provide confinement to vertical bars.

Use of reinforced concrete makes for a good composite material with extensive applications. Steel bars, however, reinforce concrete against tension only locally. Cracks in reinforced concrete members extend freely until encountering a rebar. The need for multidirectional and closely spaced reinforcement for concrete arises.

1.1.2 Fiber Reinforced Concrete

Fiber reinforced concrete is a concrete mix that contains short discrete fibers that are uniformly distributed and randomly oriented. Fiber material can be steel, cellulose, carbon, polypropylene, glass, nylon, and polyester [2]. The amount of fibers added to a concrete mix is measured as a percentage of the total volume of the composite (concrete and fibers) termed V_f . V_f typically ranges from 0.1 to 3%. Aspect ratio (l/d) is calculated by dividing fiber length (l) by its diameter (d). Fibers with a non-circular cross section use an equivalent diameter for the calculation of aspect ratio.

This research focuses on steel fibers. Steel fiber length ranges from 1/4 to 3 inches (1.5 to 75 mm) and aspect ratio ranges from 30 to 100. Fiber shapes are illustrated in Figure 1.1 [3]. The effects of steel fibers on mechanical properties of concrete are depicted in Figure 1.2 [3]. As shown in the Figure, addition of steel fibers does not significantly increase compressive strength, but it increases the tensile toughness, and ductility. It also increases the ability to withstand stresses after significant cracking (damage tolerance) and shear resistance.

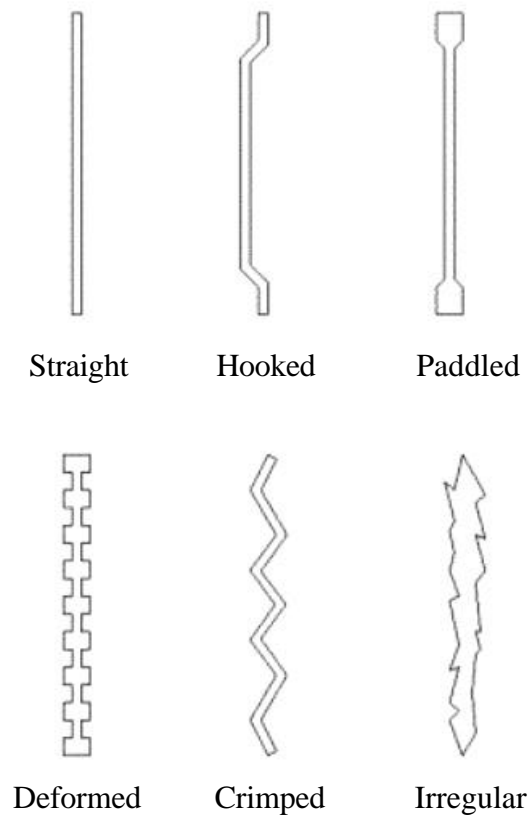


Figure 1.1 Shapes of steel fibers

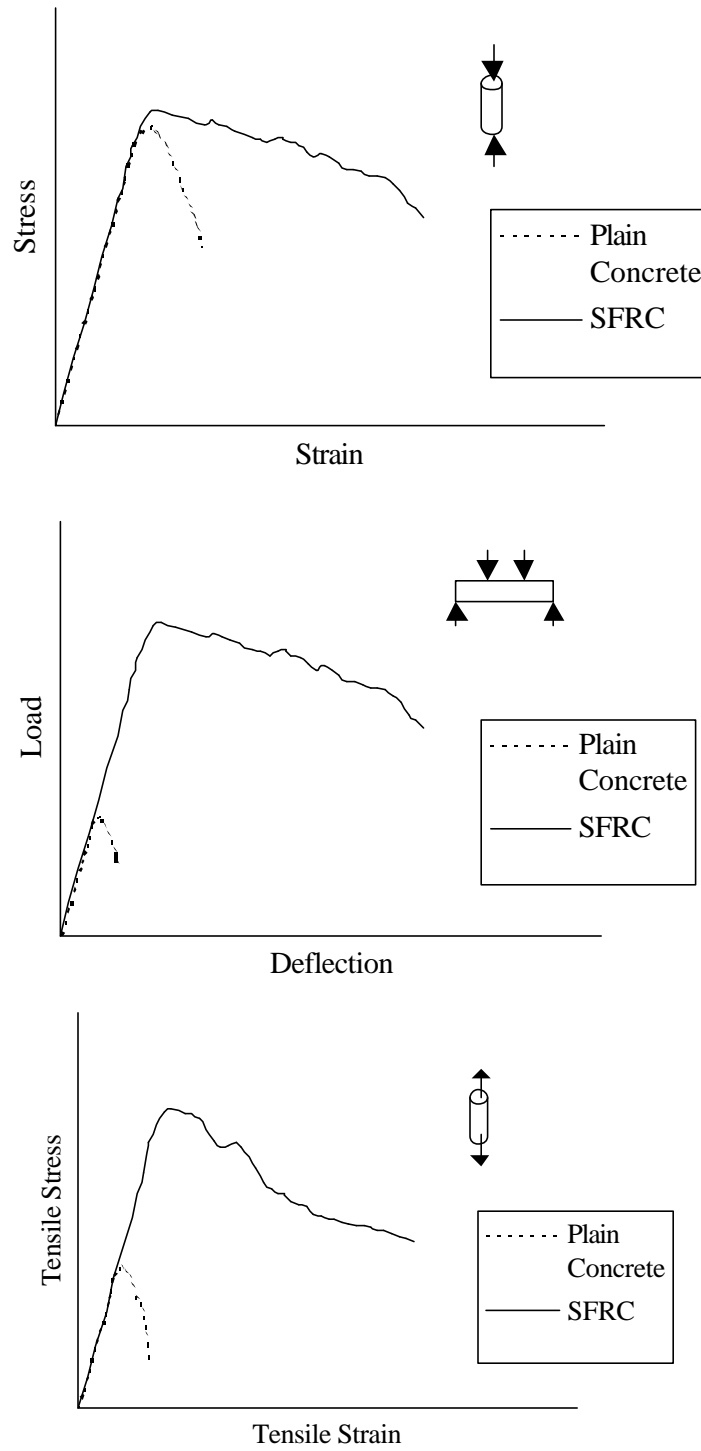


Figure 1.2 Properties of SFRC

1.1.2.1 Toughness. Toughness enhancement is among the most important contributions of steel fibers to concrete. Toughness or energy absorption capacity is the area under a load-deflection, moment-rotation, or stress-strain curve, as shown in Figure 1.3. This is especially important for structures subjected to large energy inputs such as earthquakes, blast loads, impact loads, and other dynamic loads.

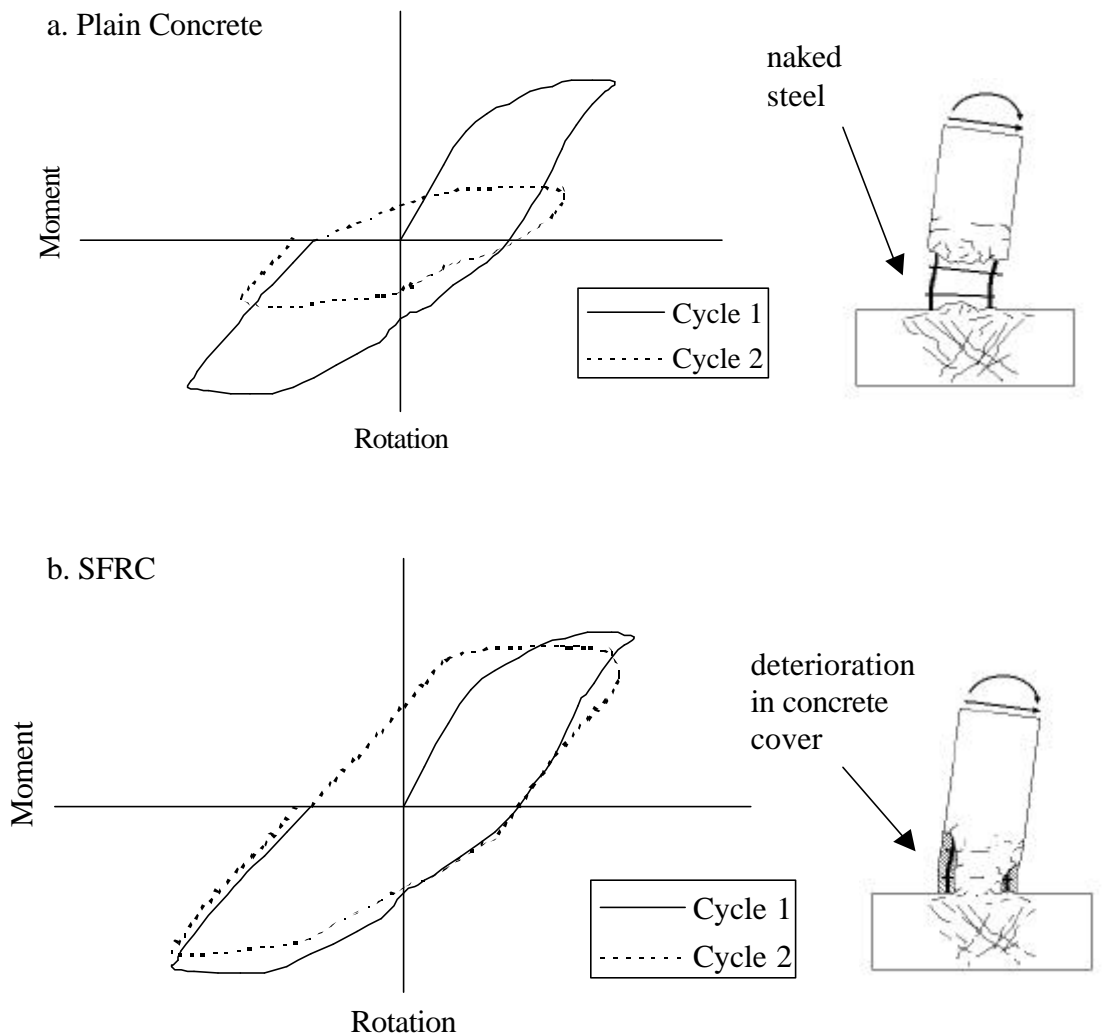


Figure 1.3 Improvements in joint behavior resulting from SFRC

1.1.2.2 Fiber Mechanisms. Fibers work with concrete utilizing two mechanisms: the spacing mechanism and the crack bridging mechanism. The spacing mechanism requires a large number of fibers well distributed within the concrete matrix to arrest any existing micro-crack that could potentially expand and create a sound crack. For typical volume fractions of fibers, utilizing small diameter fibers or micro fibers can ensure the required number of fibers for micro crack arrest.

The second mechanism term crack bridging requires larger straight fibers with adequate bond to concrete. Steel fibers are considered a prime example of this fiber type that is commonly referred to as large diameter fibers or macro fibers. Benefits of using larger steel fibers include impact resistance, flexural and tensile strengths, ductility, and fracture toughness [4].

1.1.2.3 Bridging Action. Pullout resistance of steel fibers (dowel action) is important for efficiency. Pullout strength of steel fibers significantly improves the post-cracking tensile strength of concrete. As an SFRC beam or other structural element is loaded, steel fibers bridge the cracks, as shown in Figure 1.4. Such bridging action provides the SFRC specimen with greater ultimate tensile strength and, more importantly, larger toughness and better energy absorption. An important benefit of this fiber behavior is material damage tolerance. Bayasi and Kaiser [5] performed a study where damage tolerance factor is defined as the ratio of flexural resistance at 2-mm maximum crack width to ultimate flexural capacity. At 2% steel fiber volume, damage tolerance factor according to Bayasi and Kaiser was determined as 93%.

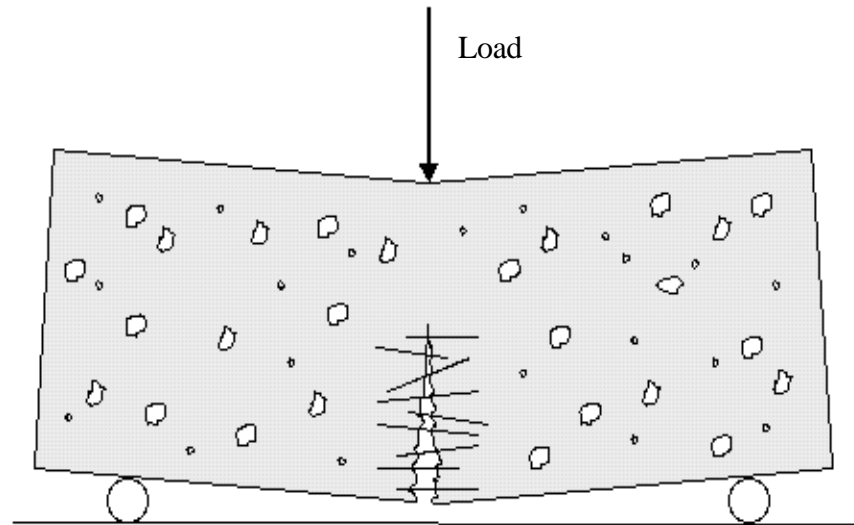


Figure 1.4 Bridging action of steel fibers

1.1.2.4 Workability. A shortcoming of using steel fibers in concrete is reduction in workability. Workability of SFRC is affected by fiber aspect ratio and volume fraction as well the workability of plain concrete. As fiber content increases, workability decreases. Most researchers limit V_f to 2.0% and l/d to 100 to avoid unworkable mixes. In addition, some researchers have limited the fiber reinforcement index [$V_f \cdot (l/d)$] to 1.5 for the same reason. To overcome the workability problems associated with SFRC, modification of concrete mix design is recommended. Such modifications can include the use of additives.

1.1.2.5 Bond Improvement. Soroushian and Bayasi [6] tested bars embedded in concrete blocks to examine the bond improvement gained by using SFRC. Steel fibers with a length of 2-in (50.8-mm), and an aspect ratio of 57 were added at a 2% volume fraction. It was found that local bond resistance increased by 55% and frictional resistance increased by 140%.

1.2 Problem Statement

During an intense seismic event, failure of beam-column joints can cause structural collapse and loss of life. Engineers have dealt with this over the years by decreasing joint tie spacing. However, this may not be the ideal solution to this problem. Before SFRC can be used, however, research must prove the advantages and safety of using steel fiber in seismic joints. Such use of SFRC may simplify placement of reinforcing bars and reduce congestion. This problem is addressed in this thesis by providing information to make SFRC an option in the building code.

1.3 Purpose of the Research

The purpose of this research is to expand the body of knowledge on the application of SFRC in building frames to help provide a basis for possible modifications to the building code. This thesis focuses on frame joints, particularly on the improvement in joint seismic performance by using SFRC. By adding hooked fibers, made of steel, to reinforced concrete, the joint is toughened which enables the structure to survive strong earthquakes.

1.4 Organization of the Research

Many researchers throughout the world have conducted testing of beam-column joints over the past 4 decades. The joints for this test were constructed to half scale. A quasi-static earthquake loading is used. The two hypotheses examined by this research are: (1) SFRC can improve seismic performance and (2) tie spacing can be increased without significantly sacrificing the improved seismic performance.

1.5 Limitations of the Research

Constructing the specimens at half-scale, is a limitation, but it is commonly done by researchers as it has been found to produce good results. The type of joint (exterior) constructed also is a limitation. There are several other possible beam-column joints that could have been tested, such as interior joints, and knee joints. The last major limitation is the ability to simulate earthquake loading using a quasi-static rate. These matters are addressed in Chapter 3.

CHAPTER 2

LITERATURE REVIEW

The literature shows that the benefits of using steel fibers in seismic joints include:

- Ductility and toughness
- Damage tolerance against multiple load cycles
- Shear resistance

The literature also shows that such benefits are provided by mechanisms that include:

- Steel bar confinement
- Dowel action improvement
- Crack bridging action
- Progressive fiber pull-out resistance

2.1 Benefits of Steel Fibers

Several researchers have explored steel fiber benefits in the seismic performance of beam-column joints. The following sheds light on these benefits.

2.1.1 Ductility and Tensile Toughness

Earthquake loading is best represented by a burst of energy applied to structures. In conventional joints, such energy is dissipated by concrete cracking, steel deformation, steel bending etc. In steel fibrous joints, the goal is to dissipate such energy via progressive fiber pullout from concrete.

In 1974, Henager was the first to publish a paper on testing of steel fiber reinforced concrete beam-column joints [7]. Two full-scale joints were constructed. One joint was built according to ACI 318-71. The other joint reduced steel congestion common in seismic

resistant joints by replacing hoops with steel fiber concrete. Brass plated steel fibers with a length of 1.5-in (38-mm) and an aspect ratio of 75 were added to the concrete mix at a volume fraction of 1.67%. An earthquake loading was simulated using a quasi-static loading rate utilizing an applied double acting hydraulic actuator. It was found that the steel fiber reinforced concrete joint had a higher ultimate moment capacity, had better ductility, was stiffer, and was more damage tolerant. Henager concluded that hoops, in the joint, could be replaced with steel fibers. Henager also concluded that SFRC could provide for a more cost effective joint.

In 1986, Lakshmipathy, and Santhakumar presented results of SFRC frame testing conducted at Anna University, in India [8]. Two frames, representing a 7 level single bay frame, were constructed at 1/4 scale; one frame was made out of reinforced concrete and the other out of SFRC. Fibers with a length of 1.57-in (40-mm) and an aspect ratio of 100 were used at a volume fraction of 1%. An earthquake loading was simulated by applying load via hydraulic jacks at the 7th, 5th and 3rd levels of the frame. It was found that the SFRC frame had a ductility increase of 57% and a 130% increase in cumulative energy dissipation in comparison to the conventional joint.

In 1987, Jindal and Sharma published results of testing SFRC knee-type beam-column connections [9]. Ninety-two knee type connections and eight conventional beam-column joint connections were tested. The parameters varied were moment to axial load ratio, type of steel fibers, volume fraction (from 0.5% to 2%), and aspect ratio of the fibers. Brass-coated high strength steel fibers of length 1-in (25.4-mm), 0.5-in (12.7-mm), and 1-in (25.4-mm), with respective aspect ratios of 100, 83.3, and 62.5 were used. Mild steel fibers of length 0.11-in (2.8-mm), 0.28-in (7-mm), 0.55-in (14-mm), 0.83-in (20.9-mm), 1.1-in

(27.9-mm), with respective aspect ratios of 10, 25, 50, 75, and 100 were used. It was found that the ultimate rotation capacity of the SFRC joints improved over the conventional joint by a factor of 6 to 9. Moment capacity was found to increase 15% to 30% as the fiber content increased to 2%. The moment capacity was also found to increase by 50% when the aspect ratio was increased from 10 to 100.

In 1988, Olario, Ioani and Poienar presented results of testing on steel fiber beam-column joints built according to the Romanian Building Code [10]. Six joints with steel fibers of varying fiber content from 0.5% to 1.5%, and two plain concrete joints were tested. The fibers used were stainless, straight, round, had a length of 1 to 1.18-in (25 to 30-mm) and a diameter of (0.38-mm). The test purpose was to analyze the influence of steel fiber reinforced concrete on stiffness, ultimate joint strength, cracking, final ductility, bond of bars, and energy dissipation. It was found that fibrous joints had a ductility increase up to 30% and an energy dissipation increase up to 46%. It was also found that stiffness as well as bond of longitudinal bars to the joint core improved.

In 1989, Gefken and Ramey published results regarding the application of steel fiber concrete in seismic joints with increased hoop spacing [11]. Straight, 1-in (25-mm) long brass-coated steel fibers with an aspect ratio of 62.5% were used at a volume fraction of 2%. The joints were designed to meet the ACI requirements for seismic joints. The fiber concrete joints were found to have a higher ultimate strength and a higher residual strength than the plain ones. It was also found that the fiber concrete joints had better energy dissipation, ductility, and stiffness, as well as less spalling than the plain concrete joints. It was also concluded that hoop spacing could be increased by a factor of 1.7 as compared to hoop spacing specified by the ACI-ASCE Committee 352. The final conclusion of Gefken and

Ramey was that by using steel fiber concrete, a type 1 joint (non-seismic) could replace a plain type 2 joint (seismic).

In 1991, Soubra, Wight, and Naaman published results of testing fiber reinforced concrete for pre-cast construction [12]. Six specimens with 2 pre-cast beam sections and one cast in place fiber joint were tested. By using fiber concrete in the cast-in-place joint, the researchers aimed to develop a seismic joint that is strong and ductile. Usage of pre-cast concrete beams and columns is rare in seismic areas because of its poor earthquake performance history and a lack of design recommendations for connections. Hooked steel fibers with a length of 1.2-in (30-mm) were used at volume fractions of 4% and 2.1%. Hooked steel fibers with a length of 2-in (50-mm) were also used at a volume fraction of 1%. No fiber diameter or aspect ratio was mentioned.

Twelve strain gages were placed on each test specimen, eight in the joint and 4 in the pre-cast beams. A universal-testing machine was used to simulate an earthquake loading for the beams under third point loading. Results showed the SFRC cast-in-place joint had larger displacement ductilities, and better energy dissipation than a conventional joint. It was concluded that testing of more realistic connections would be needed because the third point loading subjected the joint to a constant moment and no shear. A moment gradient and large shear forces are present in a joint during a seismic event.

Olario, Ioani, and Poienar published results of testing SFRC beam-column joints, including pre-cast joints [13]. Four full-scale beam-column joints and three pre-cast joints were tested. By using steel fibers in the pre-cast joints, the researchers aimed to produce a joint with less congestion, greater strength and improved energy dissipating capacities. The joints tested were designed to meet the specifications for an 8 level structure, in Romania,

according to Romanian building code. Steel fibers with a length of 1.78-in (45-mm) and an aspect ratio of 118 were used. It was concluded that the pre-cast SFRC joint was superior to the conventional joint because of its higher ultimate strength capacity. It was also found that the SFRC joint had better confinement, better control of cracking, and lower stiffness degradation. For one of the SFRC specimens, the energy dissipating capacity was 50% greater than the conventional pre-cast joint. This testing allowed the researchers to finish Romanian design provisions for the usage of SFRC in seismic joint design.

2.1.2 Damage Tolerance against Multiple Load Cycles

Earthquake causes seismic joints to be subjected to multiple cracking in reverse cycles of loading. Conventional concrete loses its resistance completely after cracking. However, fiber concrete can sustain a portion of its resistance following cracking to resist more cycles.

In 1987, Sood and Gupta, published results on the behavior of steel fibrous concrete beam-column connections [14]. Round, mild steel fibers with a length of 1.24-in (31.5-mm), and an aspect ratio of 100 were used at volume fractions of 0.6%, 0.8% and 1%. A total of 50 connections were tested in order to test the 3 main types of connections found in a multistory reinforced concrete structure. Twenty tee type, ten cross type, and twenty knee type joints were tested. Static loading (to failure) or a slow cycle fatigue load was applied to the specimens. Results showed that steel fiber concrete decreased crack width, reduced spalling, increased load carrying capacity and improved ductility.

2.2 Mechanisms

The foregoing benefits of SFRC result largely from the following properties of SFRC compared to conventional concrete.

2.2.1 Shear Resistance

Large earthquakes result in high shear forces within the beam-column joint. To withstand such forces, hoop spacing is decreased within the joint region. This can sometimes result in congestion problems that can result in construction difficulty. SFRC can be used with increased hoop spacing to provide higher shear resistance.

Craig, McConnell, Germann, Dib, and Kashani, in 1984, examined the shear behavior of 21 short columns under double curvature bending [15]. The steel fibers used had a length of 1.18-in (30-mm), an aspect ratio of 60 and were used at volume fractions of 0.75% and 1.5%. It was found that the failure mode changed from explosive to ductile as steel fiber content increased.

In 1984, Jindal and Hassan found that the shear resistance of SFRC joints was greater than that of conventional joints [16]. Steel fibers with a length of 1-in (25-mm), and an aspect ratio of 100 were used at a volume fraction of 2%. It was observed that SFRC increased the shear and moment capacities by 19% and 9.9% respectively. It was also observed that the failure mode for SFRC specimens was ductile.

In 1987, Fattuhi published results of testing conducted on SFRC corbels [17]. Corbels have the same problem as beam-column joints: joint bar congestion. Fattuhi tested twenty-two corbels to determine the improvement in shear strength gained by using SFRC or by replacing hoops with SFRC. Brass coated fibers with a length of 1.6-in (40-mm) and an

aspect ratio of 100 and doubly indented fibers with a length of 2.4-in (60-mm) length and an aspect ratio of 92.3 were used. These two types of steel fibers were used at volume fractions of 0.5%, 1% and 1.5%. Results showed a significant increase in the shear strength of the corbel. For a volume fraction of 1%, the shear strength increased by over a factor of 3. It was also found that the SRFC corbels did not exhibit the same failure mode as plain corbels, which was a catastrophic failure. Fattuhi concluded that further investigation would be needed to determine if steel fibers could replace corbel stirrups.

Narayanan and Darwish, in 1987, tested 49 simply supported rectangular beams to study the effectiveness of SFRC as shear reinforcement, and to study the replacement of stirrups by steel fibers [18]. Crimped steel fibers with a length of 1.18-in (30-mm) and an aspect ratio of 100 and fibers with a length of 1.57-in (40-mm) and an aspect ratio of 133 were used at volume fractions ranging from 0.25% to 3%. It was found that for a volume fraction of 1% steel fibers, ultimate shear strength increased by up to 170% due to the crack-arresting mechanism of fibers.

In 1992, Jiuru, Chaobin, Kaijian, and Yongcheng published results of testing SFRC joints, conducted at Southeast University of China, in Nanjing, China [19]. Five exterior joints and 7 interior joints were tested under reverse cyclic loading with the goal of providing data to verify a method for calculating joint shear strength of SFRC. Steel fibers, manufactured in their laboratory by cutting round high strength steel wire, had a length of 1.97-in (50-mm) to 2.16-in (55-mm) and an aspect ratio of 66 to 75. Shearing thin low-carbon steel plates manufactured steel fibers, with a length of 1-in (25-mm) to 1.18-in (30-mm) and an aspect ratio (equivalent) of 54 to 62, with a blade. The steel fibers were used at

a volume fraction of 1.2% to 1.5%. Strain gages mounted on SFRC joint beam bars showed that the strains were lower than that of the conventional joint. This action was believed by the researchers to be the result of steel fibers carrying shear stresses. It was also found that the joint had better ductility, better energy absorption and an increased first crack strength.

In 1994, Filiatrault, Ladicani, and Massicotte reported testing of a fiber reinforced concrete joint. The volume fraction of steel fibers was 1.2% to 1.5%. The joint showed better ductility, better energy absorption and an increased first crack strength. The joint was tested under shear and the results showed that the joint had better ductility, better energy absorption and an increased first crack strength. The joint was tested under shear and the results showed that the joint had better ductility, better energy absorption and an increased first crack strength.

with a length of 2-in (50-mm) and an aspect ratio of 100 were used at a volume fraction of 1.6%. By using SFRC, the researchers hoped to verify previous results and show that a less costly and easier to construct joint would meet the weak beam-strong column philosophy.

The SFRC joint was found to have higher shear strength than the probable shear capacity for the joint built with full seismic details. It was also found that the full seismic detailed specimen dissipated more energy than the SFRC specimen. The SFRC joint dissipated 85% of the energy of the full detailed joint, whereas the undetailed joint dissipated 70% of the energy for the detailed joint. Finally, it was concluded that an SFRC joint is a possible alternative to a conventional joint.

2.2.2 Dowel Action

Beam testing conducted by Narayanan and Darwish, as discussed in the previous section, revealed that the dowel resistance was enhanced by the presence of steel fibers. The fibers improved the dowel resistance because of the increased tensile strength of the concrete in the splitting plane along the bars.

The effectiveness of SFRC on bearing stress of a concrete footing was published by Soroushian and Bayasi [22]. Test specimens consisted of concrete blocks reinforced with dowel bars and a top layer of SFRC. The steel fibers had a length of 2-in (50.4-mm), an aspect ratio of 57, and were used at a volume fraction of 2%. A quasi-static load rate was applied to the test specimens using a hydraulic compression machine. It was concluded that using SFRC for the full depth or for just the top layer, underneath the bearing pressure, could improve the ductility. It was also concluded that SFRC could increase the bearing strength, which would improve the effectiveness of dowel bars.

2.2.3 Bar Confinement

Confinement of the rebar in a seismic beam-column joint is very important for the performance of the joint in an earthquake. The bond between concrete and rebar is affected by the amount of steel congestion in a joint. If there are a lot of hoops overlapping with small spacing in a joint, then the bond between concrete and rebar can be poor. Poor bonds result when because there is not enough space between the bars to allow the concrete to pass through.

A joint with increased hoop spacing will have better bar confinement, as there will be ample room for the concrete to flow around the bars and to properly bond. However, in a seismic beam-column joint it can be nearly impossible to allow for an increased hoop spacing to provide better confinement because the high shearing forces present in a joint require numerous hoops. To remedy this situation, steel fiber concrete can be used in place of some hoops.

In 1984, Craig, Mahadev, Patel, Viteri, and Kertesz reported testing of half-scale seismic beam-column joints to show that SFRC can produce a more seismic resistant joint [23]. Two variations of hooked end steel fibers were used at a volume fraction of 1.5%. One of the variations had a length of 1.18-in (30-mm) and an aspect ratio of 60. The other had a length of 1.97-in (50-mm) and an aspect ratio of 100. It was found that a joint with hooked end steel fibers provided better confinement than a plain concrete reinforced joint. It was also found that the SFRC joints had less structural damage, had a greater shear capacity, greater stiffness, and had approximately 15% increase in maximum moment at each ductility factor.

CHAPTER 3

EXPERIMENTAL PROGRAM

This chapter describes the experimental program that was designed to explore the hypotheses made by this thesis.

3.1 Objectives

The objectives for this experiment were to demonstrate that a concrete mix with a 2% volume fraction of hooked end steel fibers could allow hoop spacing in a seismic beam-column joint to be increased. The SFRC joint was required to be comparable in toughness to a conventional joint with hoop spacing as specified by the 1997 UBC. These objectives were fulfilled by the experimental program and described in this chapter.

3.2 Plan

To meet the objectives of this experiment, six beam-column joints were constructed to a half-scale. Test fixtures, test specimens, and seismic loading are described herewith.

3.2.1 Test Fixture

The Concrete Research Institute at San Diego State University has test fixtures, consisting of three 20-ft (6.1-m) long steel I-beams embedded in the concrete slab floor as shown in Figure 3.1. Two of the I-beams were used to anchor the half-scale models of beam-column joints, as seen in laboratory layout depicted in Figure 3.2.

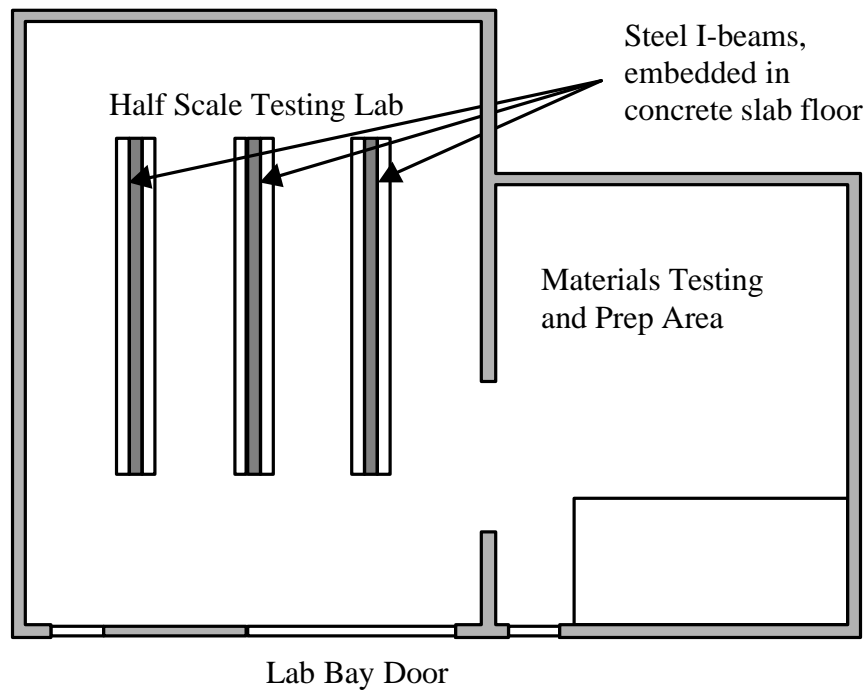


Figure 3.1 Laboratory Setup

On top of each I-beam, used as a test fixture, three beam-column joints and four strong walls were constructed as shown in Figure 3.3. Anchor bolts secured the strong walls to the I-beams by utilizing the 1/2-in (1.3-cm) apertures, in the top flange, spaced at 5-in (12.7-cm). A trough in the slab floor exposed the upper I-beam flanges so that the anchor bolts could be secured. I-beam flange width was 10-in (25.4-cm), which was also the width of strong walls, beams and columns for this experimental program.

The strong walls were 24-in (61-cm) long and 48-in (122-cm) high. Running along the top of the I-beams, was the column, which was 10-in (25.4-cm) deep and 48-in (122-cm) long. Resting on the middle of the column, was the beam. The beam was 12-in (30.5-cm) wide, 10-in (25.4-cm) deep and 38-in (96.5-cm) in height. A definition of the elements comprising a beam-column joint is shown in Figure 3.4.

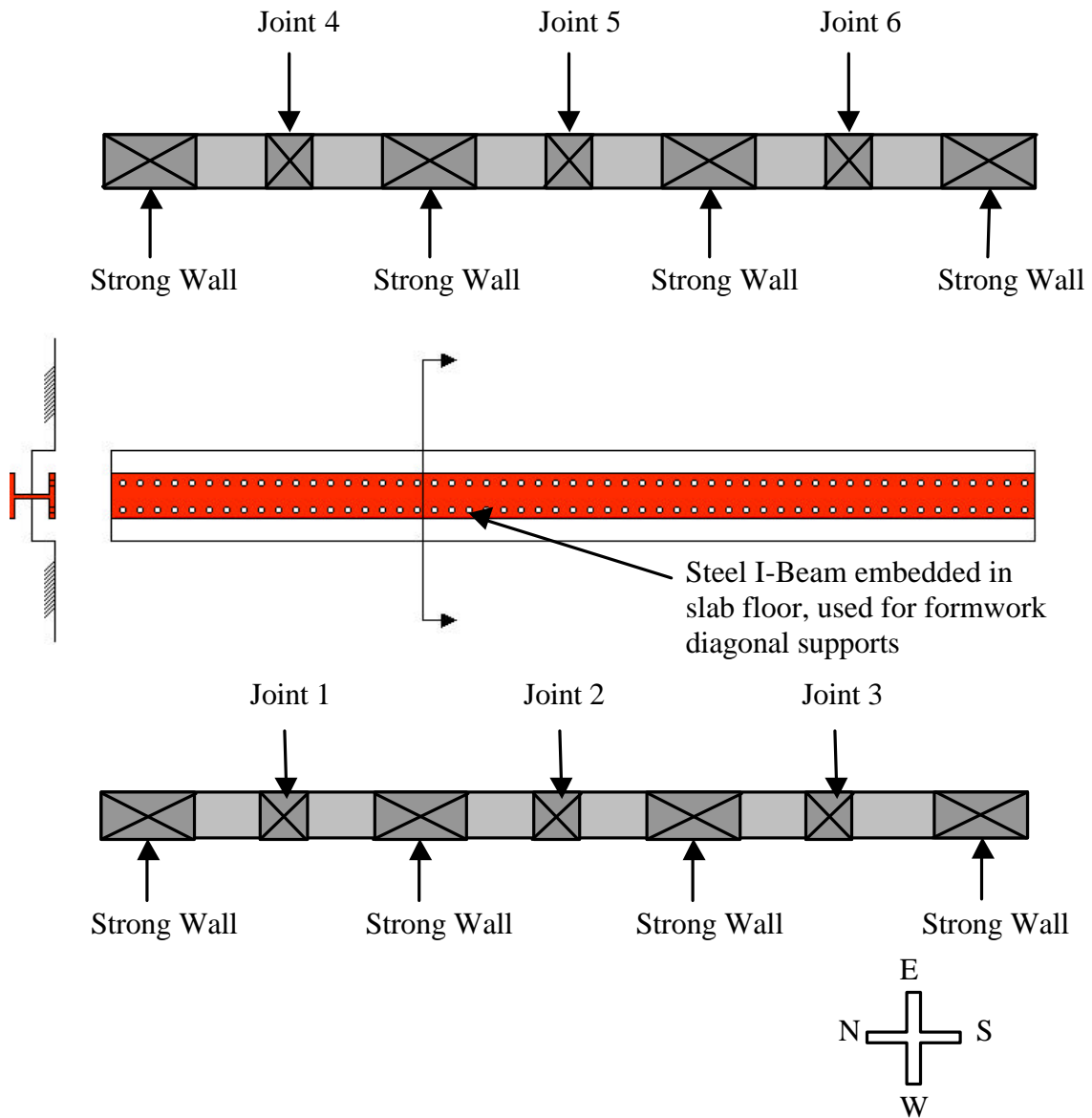


Figure 3.2 Laboratory layout of test specimens

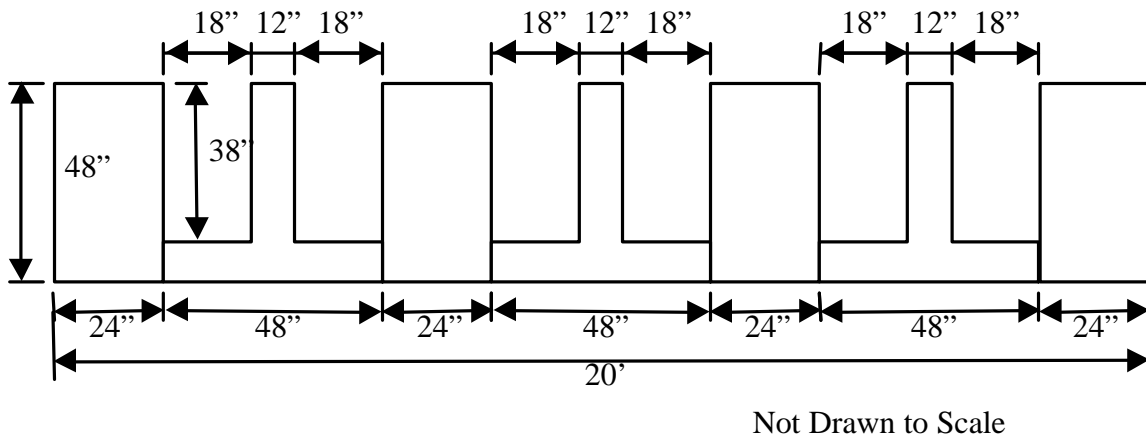


Figure 3.3 View of specimens constructed on top of each I-beam

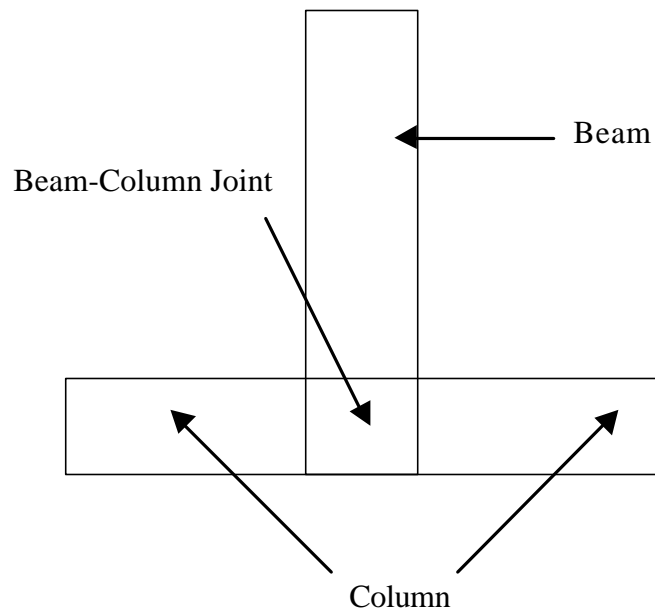


Figure 3.4 Definition of the elements comprising a test specimen for a beam-column joint

3.2.2 Load Pattern and Application

A quasi-static hysteretic earthquake loading was applied to each beam-column joint test specimen. Loading consisted of six cycles with load point maximum displacements of 1/4-in (6.35-mm), 1/2-in (12.7-mm), 1-in (25.4-mm), 2-in (50.8-mm), 4-in (101.6-mm), and 8-in (203.2-mm) for cycles 1, 2, 3, 4, 5, and 6 respectively, as shown in Figures 3.5 and 3.6. The load, applied near the top of beam, was gradually increased using displacement-controlled procedure during each loading cycle until the target deflection was reached. For each cycle, the beam was displaced to the desired amount then load was released. The joint would not return to the initial position since the beam had undergone permanent distortion. This distortion was referred to as a residual displacement. The beam was then returned to the zero displacement position before the next half-cycle began.

Load was applied utilizing hydraulic jacks. After the jack was bolted onto the strong wall loading plate, a load cell was inserted between the jack and beam, as shown in Figure 3.7.

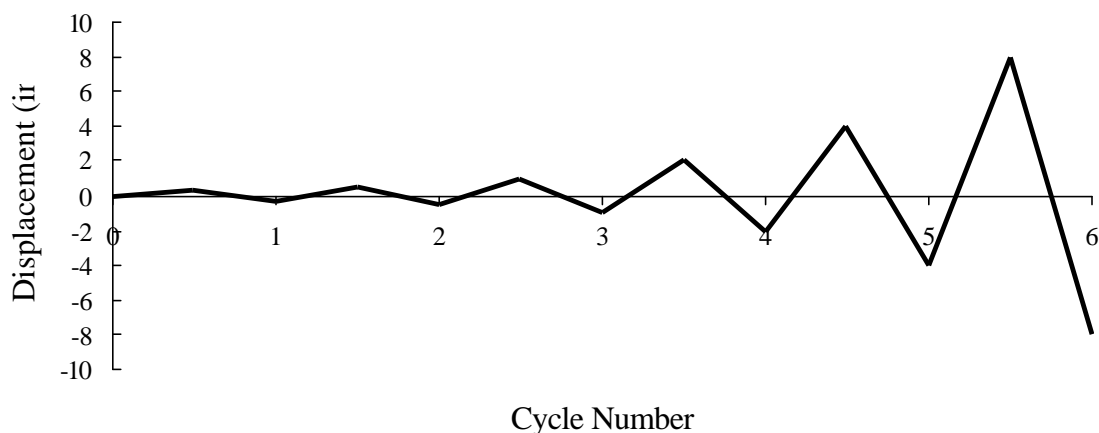


Figure 3.5 Simulated quasi-static earthquake loading

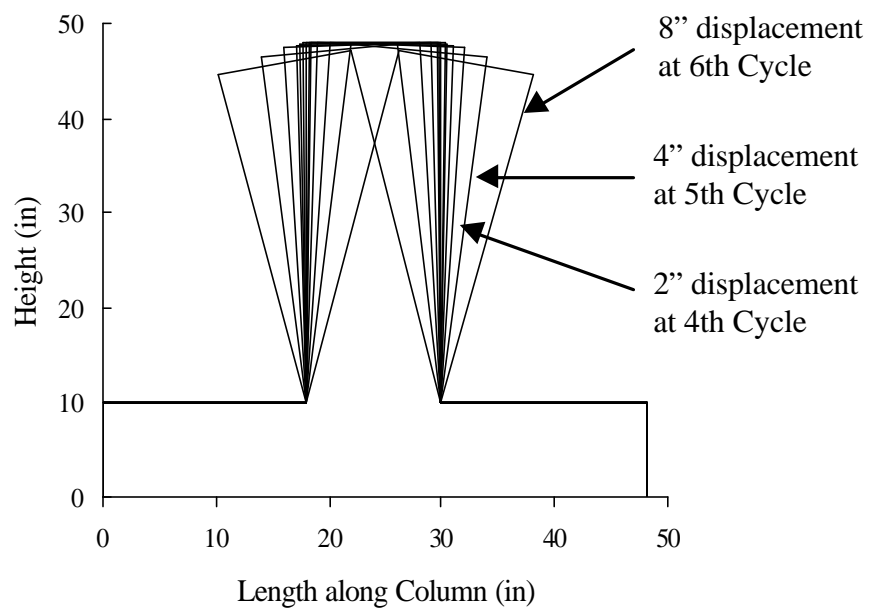


Figure 3.6 Beam displacement during simulated earthquake

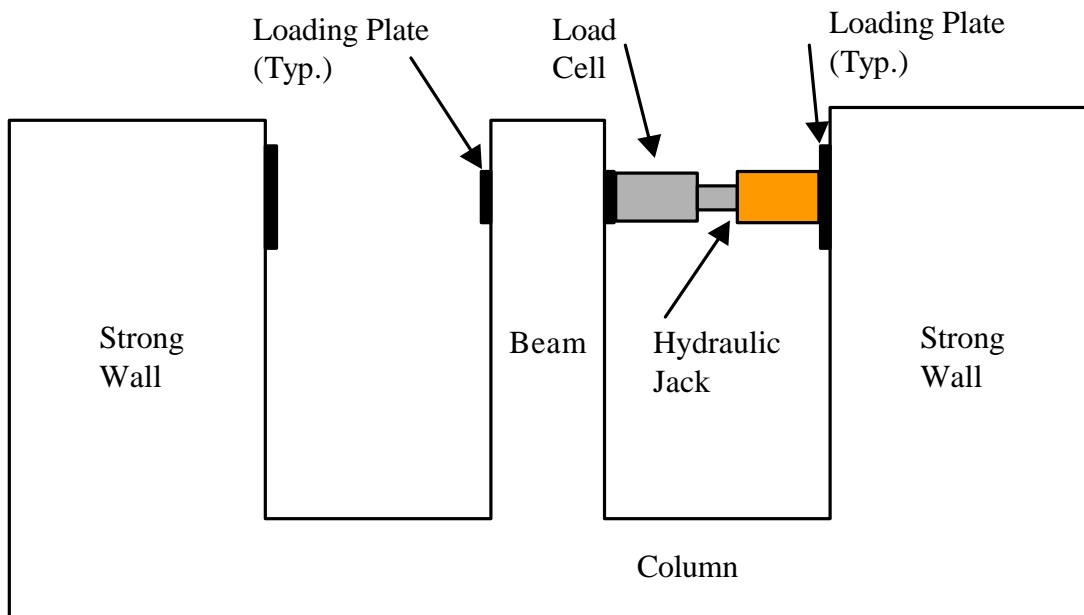


Figure 3.7 Setup of load cell and hydraulic jack

3.3 Joint Design

The design of a full-scale joint, according to the 1997 UBC is discussed in this section, as is the design of the half-scale joint used for testing.

3.3.1 Conventional Joint Design

The testing setup was designed to reflect a column with cross sectional dimensions of 15-in (38.1-cm) by 12-in (30.5-cm) and a beam of cross sectional dimensions 12-in (30.5-cm) by 24-in (61.0-cm). Figure 3.8 depicts the bar arrangement for a beam-column joint with 4-in (10.2-cm) spacing. Beam top longitudinal reinforcement was 2 #8 and 1 #6, or 2.01-in^2 (13.0-cm^2), and bottom longitudinal reinforcement was 3 #6, or 1.32-in^2 (8.52-cm^2). Column longitudinal reinforcement was 4 #7 (2.40-in^2). Ties/hoops were #3 at 4-in (10.2-cm) on center in both the column and in the beam.

3.3.2 Half-Scale Joint Design

Half scale results in a 6-in (15.2-cm) wide joint with a column depth of 7.5-in (19.1-cm) and a beam depth of 12-in (30.5-cm). The use of 10-in (25.4-cm) wide joints was done for practical purposes. For the same reason, column depth was selected to be 10-in (25.4-cm). Beam top longitudinal reinforcement was 2 #5 and #4 or 0.81-in^2 (5.2-cm^2) and bottom longitudinal reinforcement was 3 #4 or 0.60-in^2 (3.9-cm^2). Column longitudinal reinforcement was 4 #5 or 1.23-in^2 (7.9-cm^2). Ties/hoops were #2, or 0.05-in^2 (0.32-cm^2) at 4-in (10.2-cm) on center. These values are approximately equal to half of the reinforcement for the full-scale joint. Figure 3.9 depicts the bar arrangement for a typical test specimen. The bar arrangement, under construction, for a plain concrete specimen is shown in Figure 3.10.

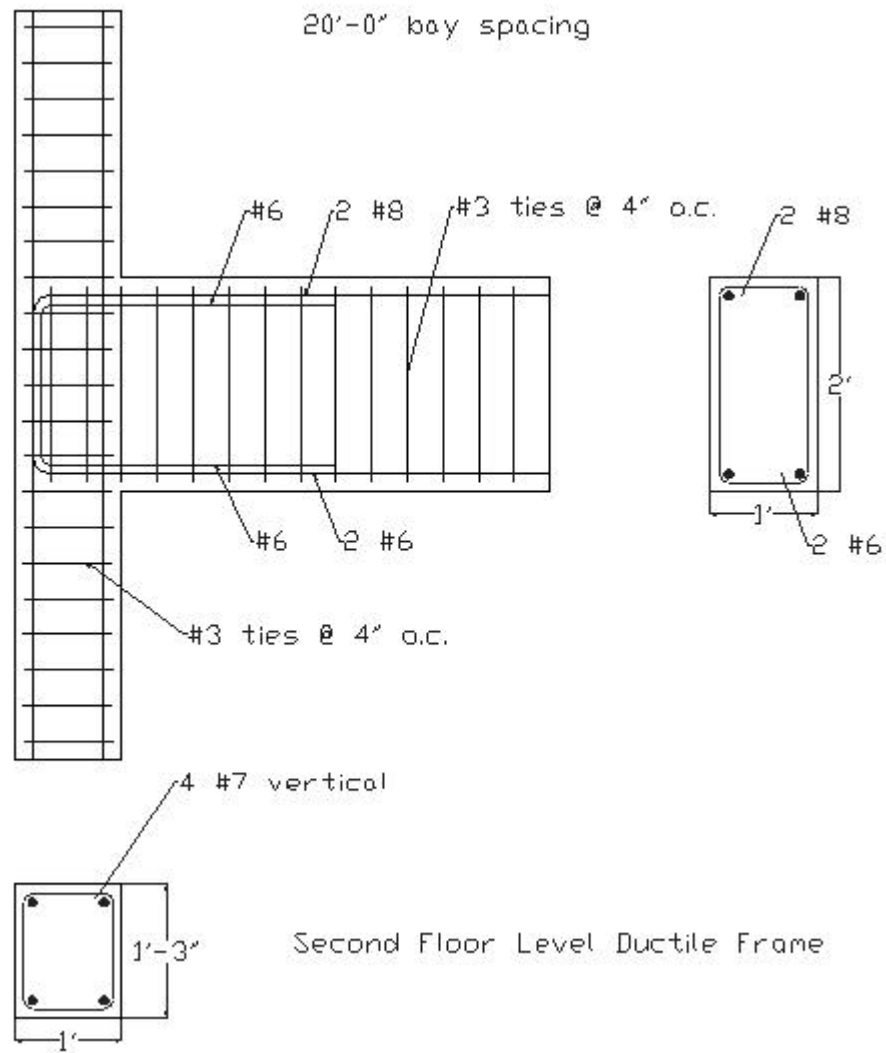


Figure 3.8 Bar arrangement for a full-scale beam-column joint

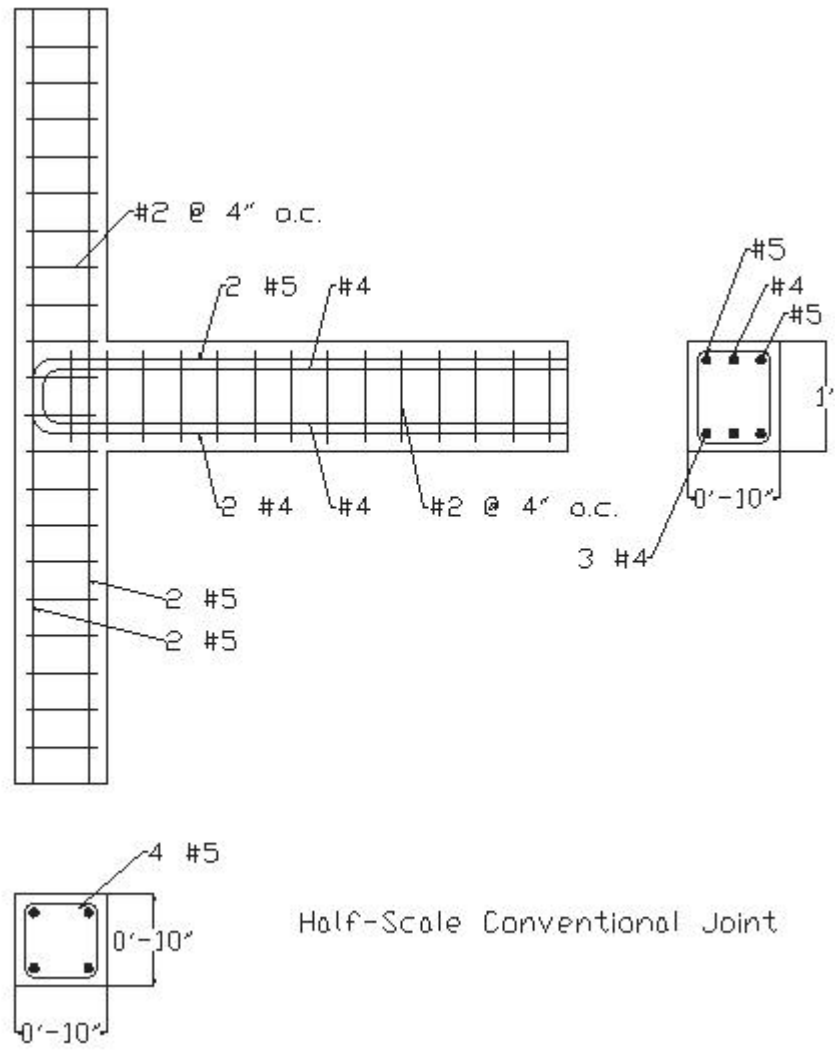


Figure 3.9 Bar arrangement for a typical test specimen



Figure 3.10 Bar arrangement under construction for a plain concrete test specimen

Joints 3 and 6 were plain concrete joints with hoop spacing of 4-in (10.2-cm). Joints 1 and 5 were steel fiber concrete joints with hoop spacing of 6-in (15.2-cm). Joints 2 and 4 were steel fiber concrete joints with hoop spacing of 8-in (20.3-cm).

3.4 Test Setup

The setup of testing equipment used to simulate and record data for a simulated quasi-static earthquake loading is discussed in this section.

3.4.1 Strain Gage Locations

A total of six strain gages were installed in each beam- column joint, as shown in Figure 3.11. Four of the gages were placed on the vertical beam steel bars approximately 1

to 2-in above the top longitudinal rebar of the column. The fifth and sixth strain gages were placed on the top and bottom longitudinal rebars, respectively, in the middle of joint.

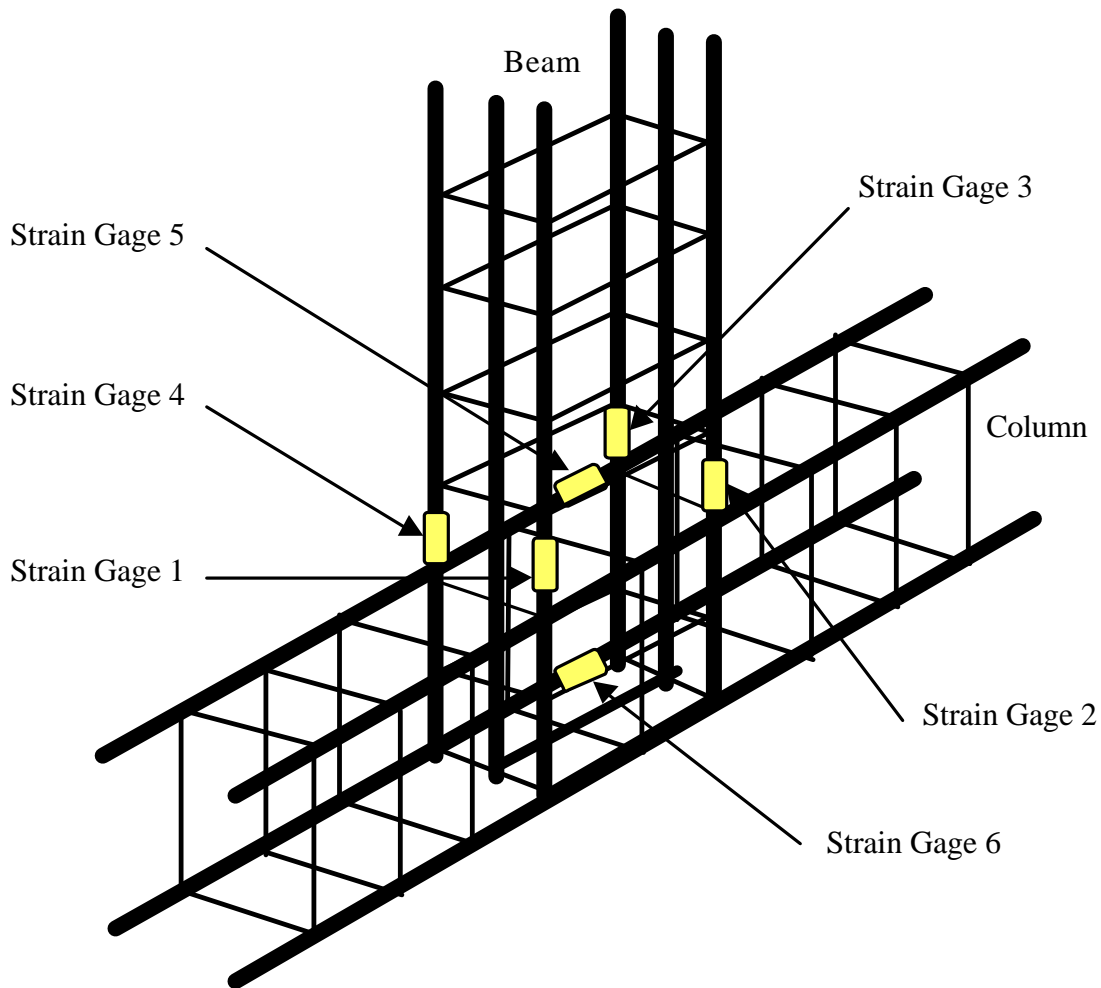


Figure 3.11 Location of strain gages on a typical test beam-column joint

3.4.2 Setup of Equipment

After the hydraulic jack was bolted to the strong wall loading plate, the loading plate was then secured to the strong wall. Next, the load cell was placed in the gap between the jack and beam. The jack was extended just enough so that the load cell would then be held in place, as depicted in Figure 3.12. The load cell and joint strain gages were then connected to

a data acquisition system which, in turn, was connected to a personal computer, as depicted in Figure 3.13 that recorded and saved the test data.



Figure 3.12 Test specimen ready for loading



Figure 3.13 Data acquisition system, PC, and test setup

3.5 Construction

Details about the loading plates, about the placement of concrete joints and about the placement of SFRC joints will be discussed in this section.

3.5.1 Loading Plates

Properly placing and securing the 1/2-in (1.27-cm) diameter, 5-in (12.7-cm) long J-bolts for the loading plates was very critical. The loading plates had to be aligned at the correct level, as shown in Figure 3.14, so that the hydraulic jack is aligned with the beam and strong wall. The jack was bolted to an 8-in (20.3-cm) square, 1/2-in (1.27-cm) thick, loading plate, that was attached to the strong wall via four J-bolts of the type mentioned above. The jack loading piston had to align with the center of a 4-in (10.1-cm) by 8-in (20.3-cm), 1/2-in (1.27-cm) thick, loading plate, that was mounted on the beam via two J-bolts. A graphic representation of a beam with a loading plate is shown in Figure 3.15. A detail of the J-bolts and reinforcing bars in a beam is shown in Figure 3.16. Figure 3.17 illustrates the configuration of loading plates and J-bolts within the strong wall. A graphic representation of a strong wall with the loading plate is illustrated in Figure 3.18. As shown, the strong wall loading plate is placed sunken within the side of the strong wall.

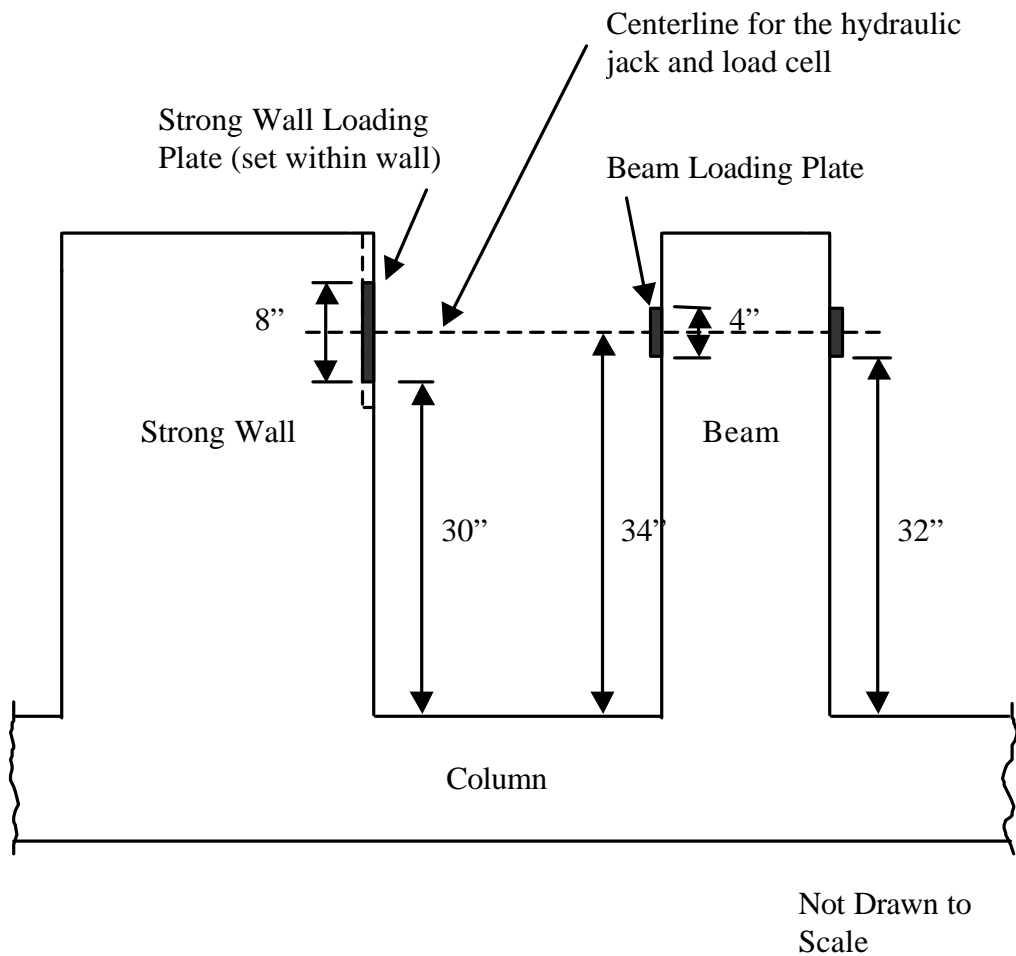


Figure 3.14 Alignment of loading plates, hydraulic jack and load cell

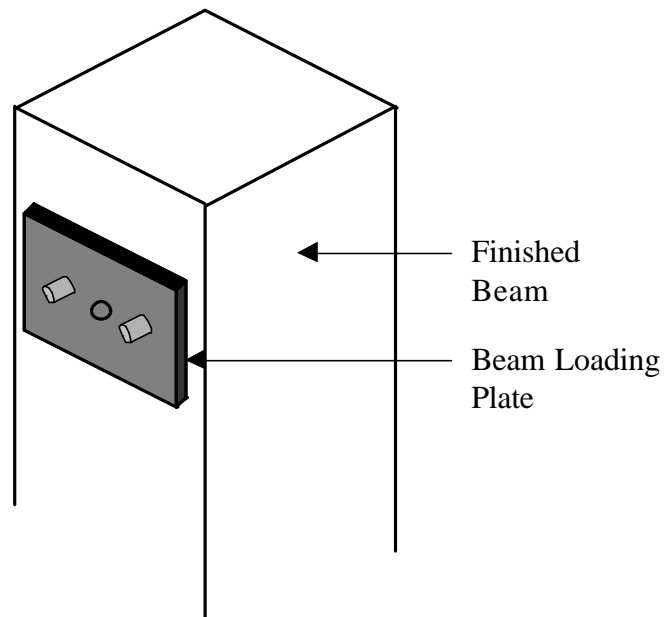


Figure 3.15 Typical test specimen ready for beam-column testing

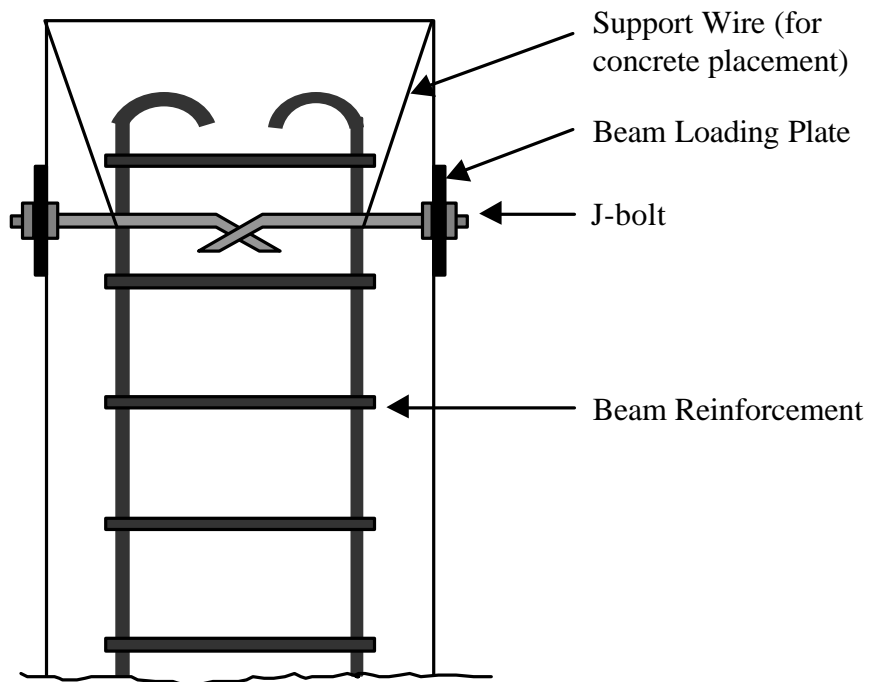


Figure 3.16 Detail of J-bolt placement in a typical beam

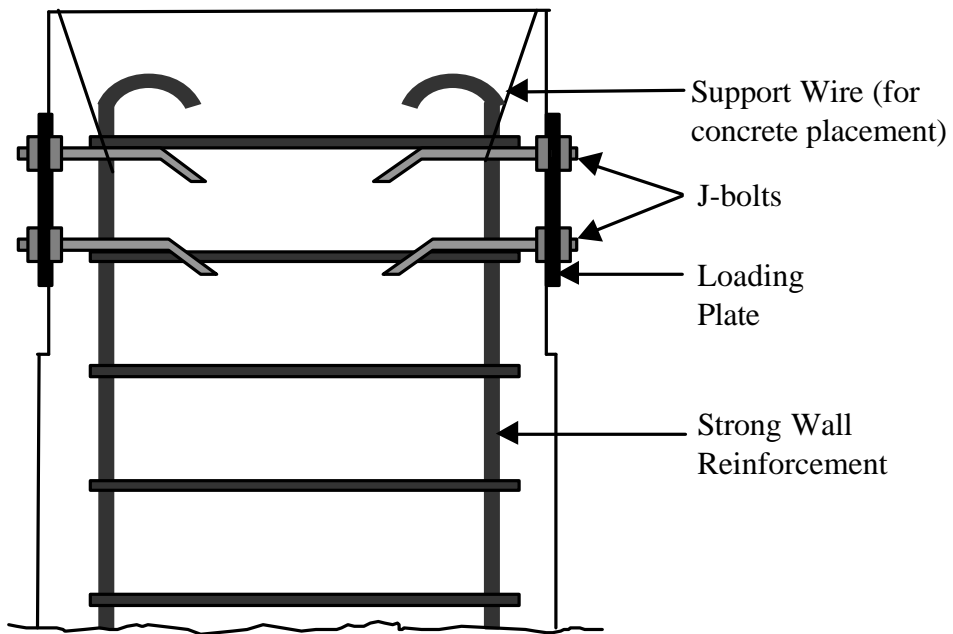


Figure 3.17 Detail of strong wall

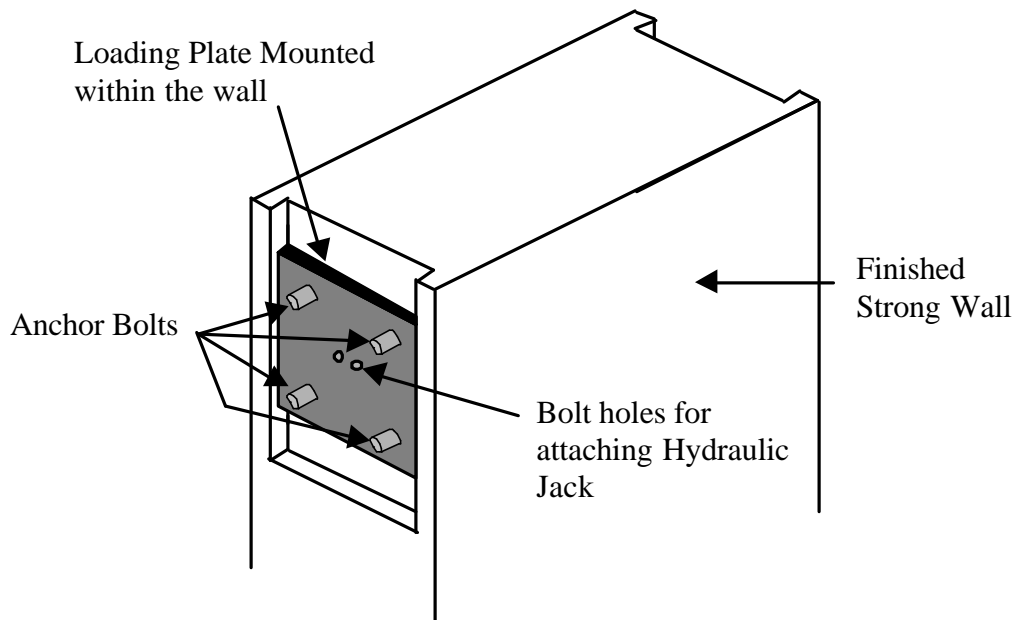


Figure 3.18 Detail of base plate embedded within strong wall

3.5.2 Placement of Concrete

Plain concrete arrived at the site in a rotary drum semi-truck. The plain concrete joints and strong walls were placed first. Shoveling and internal vibration were utilized. Following the 30 minute time required for plain concrete placement, steel fibers were added to the revolving drum mixer at the top of the chute. After the concrete was re-mixed for about 20 minutes, the steel fibrous joints and strong walls were placed also utilizing shoveling and internal vibration, as depicted in Figure 3.19. Steel fiber concrete placement took about 1 hour. General precautions listed in the American Concrete Institute Guide for specifying, mixing, placing, and finishing steel fiber reinforced concrete (1984) were followed in construction [24]. Figure 3.20 shows the test setup shortly after placement.



Figure 3.19 Internal vibration of SFRC



Figure 3.20 Test specimens shortly after concrete placement

3.6 Quality Control

Quality control tests performed on the day of joint placement for plain concrete and for SFRC are discussed in this section.

3.6.1 Fresh Concrete

Standard slump test was run for plain and steel fibrous concrete. Additionally, an air void ratio test via the pressure method, unit weight and temperature tests were also used as quality control procedures for fresh concrete. For fresh fiber concrete, as depicted in Figure 3.21, the standard inverted slump cone test was used.



Figure 3.21 SFRC

3.6.2 Hardened Concrete

Six 12-in (30.5-cm) high, 6-in (15.2-cm) diameter cylinders and six 4-in (10.2-cm) x 4-in (10.2-cm) x 14-in (35.6-cm) beams were cast of the plain and fibrous mixes of this study. Of the aforementioned samples, half was plain concrete and the other half was fibrous concrete.

3.7 Materials

Properties of materials used in this experiment will be discussed in this section. Those materials include plain concrete, SFRC, reinforcing bars, anchor bolts and strain gages.

3.7.1 Plain Concrete

The concrete mix was provided by Superior Ready Mix of San Diego County,

California. The mix contained Type II Mitsubishi cement, class F Phoenix fly ash, Master Builders Pozzoloth 332-N (water reducer), water from San Diego County, sand, and coarse aggregate with a maximum size of 3/8-in (9-mm). Crushed rock made up half of the total aggregate whereas sand made up the other half. The fineness modulus of the coarse aggregate was 5.84 and the fineness modulus of sand was 2.93.

The mix was designed for compressive strengths f'_c and f'_{cr} of 3,000-psi (21-MPa) and 4,060-psi (28-MPa), respectively. Mix design properties also included a unit weight of 142.8-pcf (2,288-kg/m³), a slump of 4-in (100-mm) and a water/ cement ratio of 0.59.

3.7.2 Steel Fibers

Dramix steel fibers manufactured by Bekaert Corporation were used at a 2% volume fraction. They were hooked-end and had a length of 1.2-in (31-mm) and a diameter of 0.020-in (0.50-mm) resulting in an aspect ratio of about 60.

3.7.3 Steel Reinforcing Bars

Grade 60 ($f_y = 60\text{-ksi} = 420\text{-MPa}$) deformed steel reinforcing bars were used for the longitudinal and lateral reinforcement. The steel reinforcing bars were detailed by Quality Reinforcing and transferred to the Concrete Laboratory where they were tied in place.

3.7.4 Anchor Bolts

The anchor bolts used to secure the strong walls to the steel I-beam embedded in the floor, had a strength of 60-ksi (420-MPa), a diameter of 1/2-in (1.27-cm), a length of 18-in (45.7-cm) and an arched end with radius of 3-in (7.6-cm). The anchor bolts used for the

loading plates were 7-in (17.8-cm) long, had a bent end that was 1-in long, and a diameter of 3/8-in. These bolts also had a yield strength of 60-ksi (420-MPa).

3.7.5 Strain Gages

Precision Strain gages manufactured by Micro Measurements Division of Measurements Group were used. The gage model is CEA-06-500UW-120. Properties include a resistance of 120.0 +- 0.3% ohms at 24°C, a gage factor of 2.085 +- 0.5% at the same temperature, and a transverse sensitivity of 0.0 +- 0.2%.

The strain gage locations, on the column rebar and on the beam rebar were sanded and cleaned using a procedure recommended by the manufacturer. The gages were carefully placed using a procedure recommended by the manufacturer. After the strain gages were placed on the steel bars, an ohmmeter was used to make sure they functioned correctly by reading a resistance of 120 ohms.

Because of the small size of the terminals, on the strain gage, 16-gauge wire was soldered to the terminals. A coaxial cable was then soldered to each of the 16 gauge leads. The leads and cables were secured to the rebar and routed down to the floor with the aide of electricians tape. This was done to protect the cables and the gages from being damaged by the placement of concrete. The strain gages were further protected by taping a small piece of styrofoam over the gage and lead connection. An electrical tape was further placed onto the styrofoam for further protection, as depicted in Figure 3.22. Once the cables reached the floor, they exited the test specimen through one of the boltholes in the steel I-beam.



Figure 3.22 Protected strain gages

CHAPTER 4

RESULTS

The main results discussed in this chapter include hysteresis loops (load versus deflection), bar strains, and material tests.

4.1 Hysteresis Loops

Hysteresis loops of load versus beam deflection, for SFRC joints #1 and #5, with 6-in (15.2-cm) spacing, are shown in Figures 4.1 and 4.2.

Hysteresis loops for SFRC joints #2 and #4, with 8-in (20.3-cm) spacing, are shown in Figures 4.3 and 4.4.

Hysteresis loops for conventional joints #3 and #6, with 4-in (10.2-cm) spacing are shown in Figures 4.5 and 4.6.

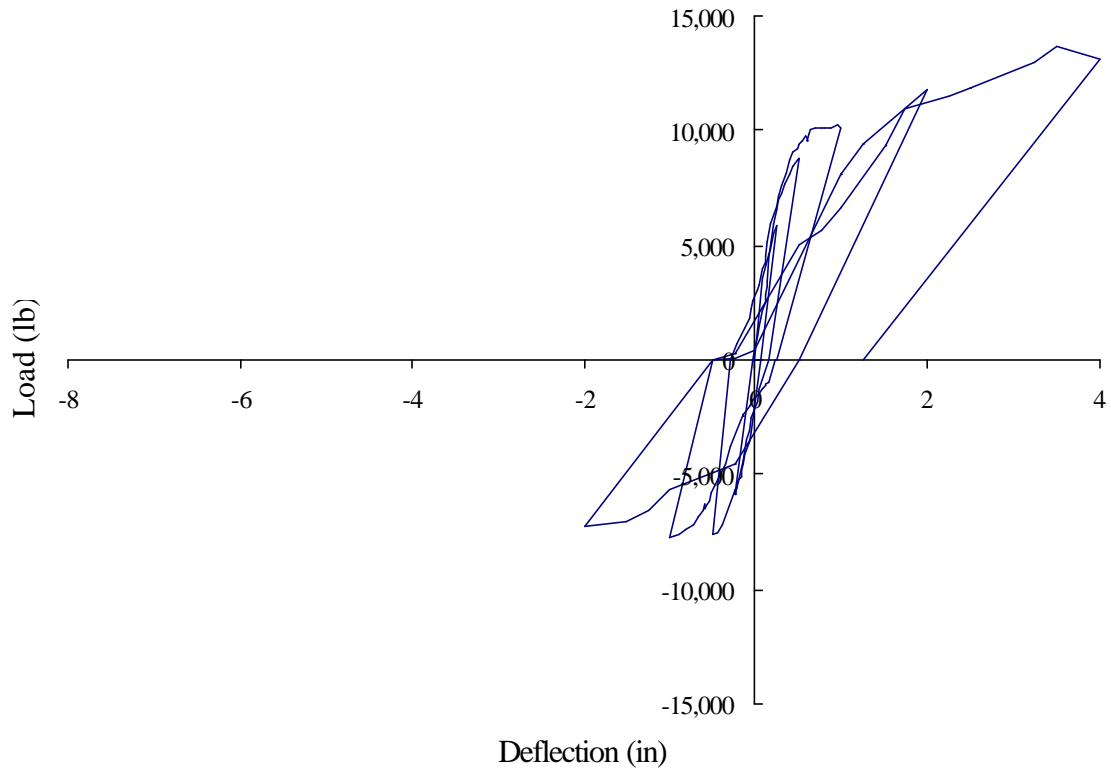


Figure 4.1 Hysteresis loop for SFRC beam-column joint #1 with 6-in (15.2-cm) spacing

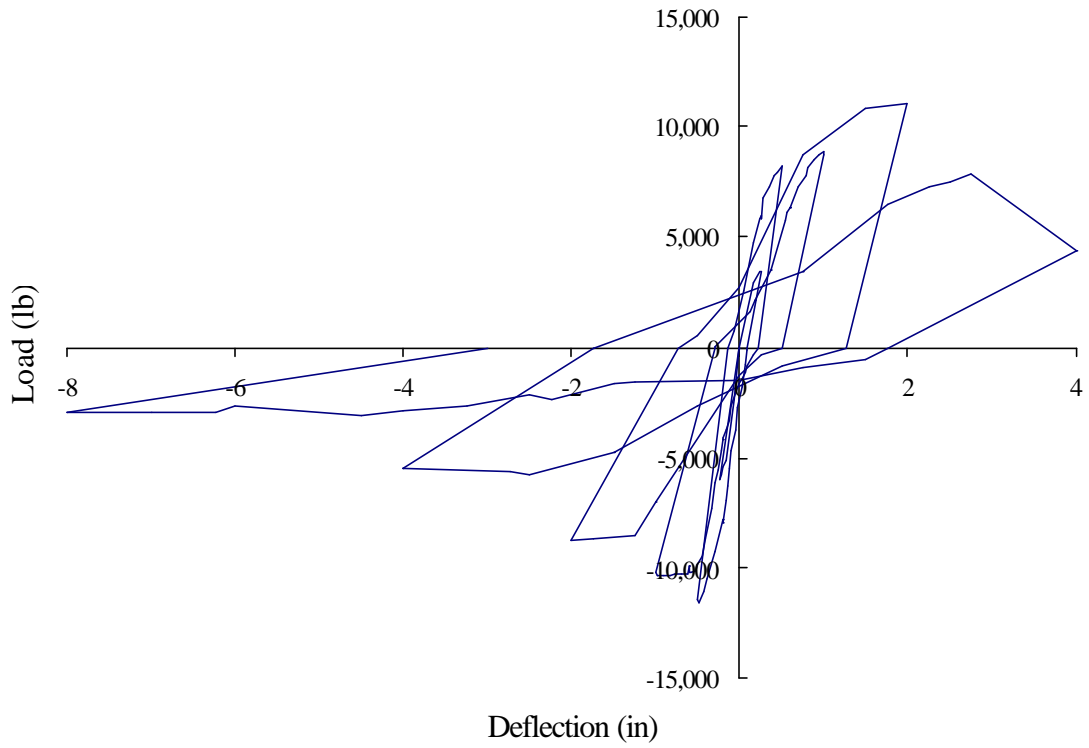


Figure 4.2 Hysteresis loop for SFRC beam-column joint #5 with 6-in (15.2-cm) spacing

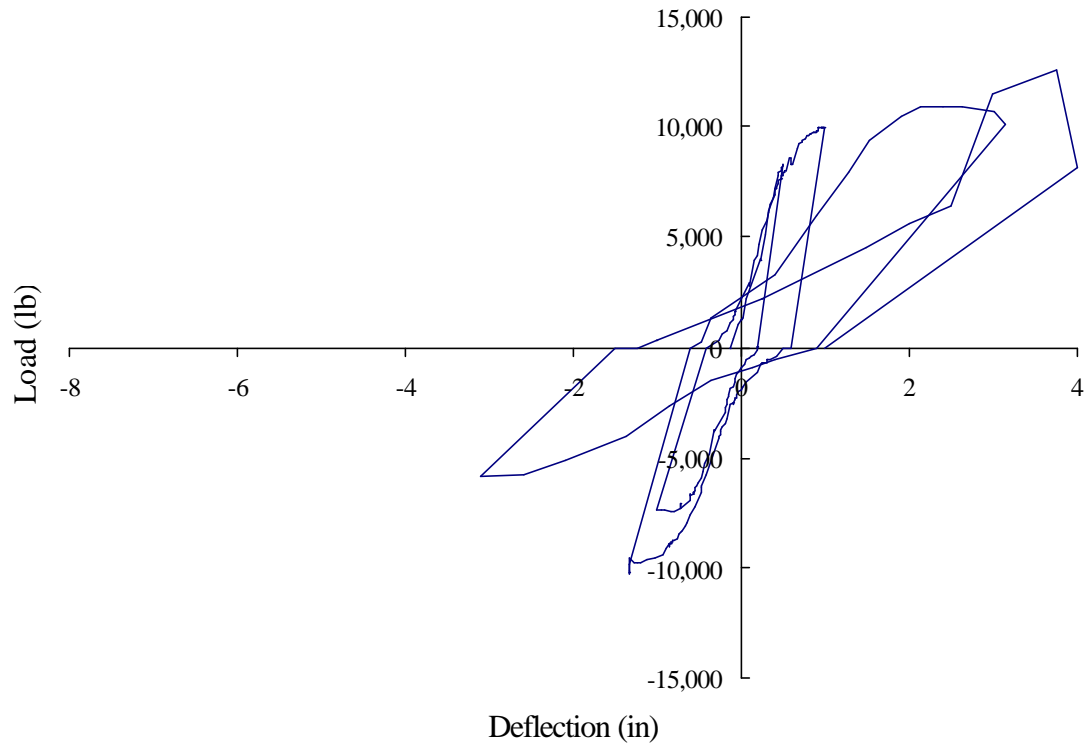


Figure 4.3 Hysteresis loop for SFRC beam-column joint #2 with 8-in (20.3-cm) spacing

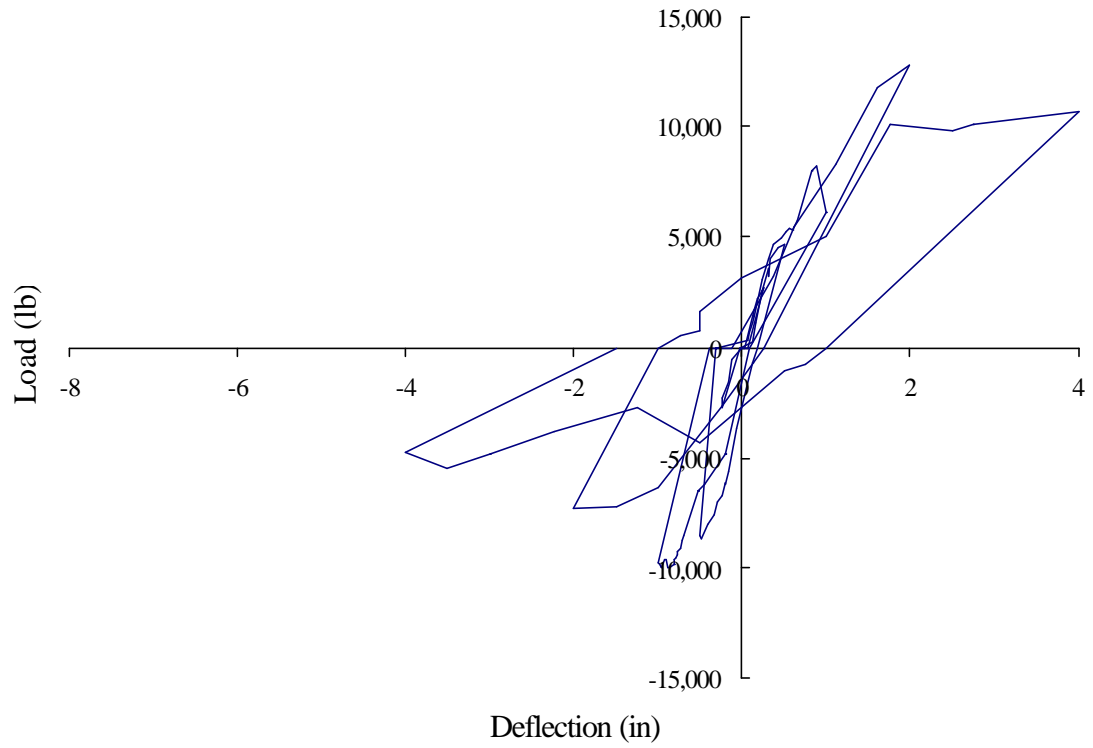


Figure 4.4 Hysteresis loop for SFRC beam-column joint #4 with 8-in (20.3-cm) spacing

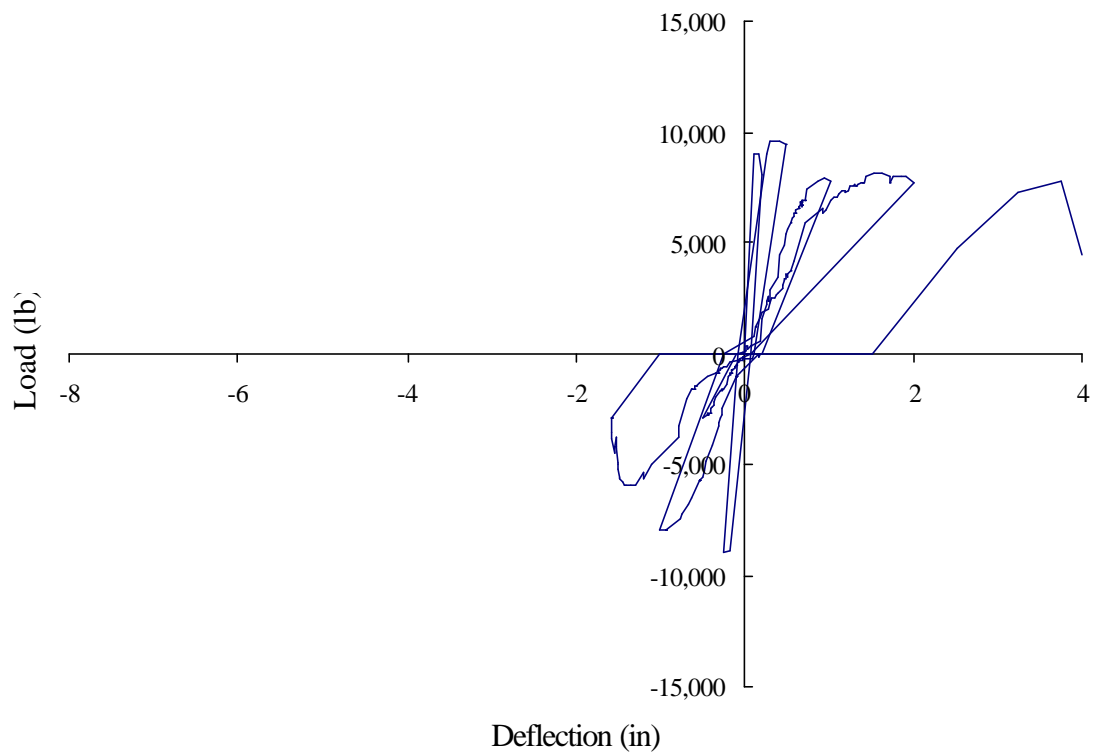


Figure 4.5 Hysteresis loop for plain beam-column joint #3 with 4-in (10.2-cm) spacing

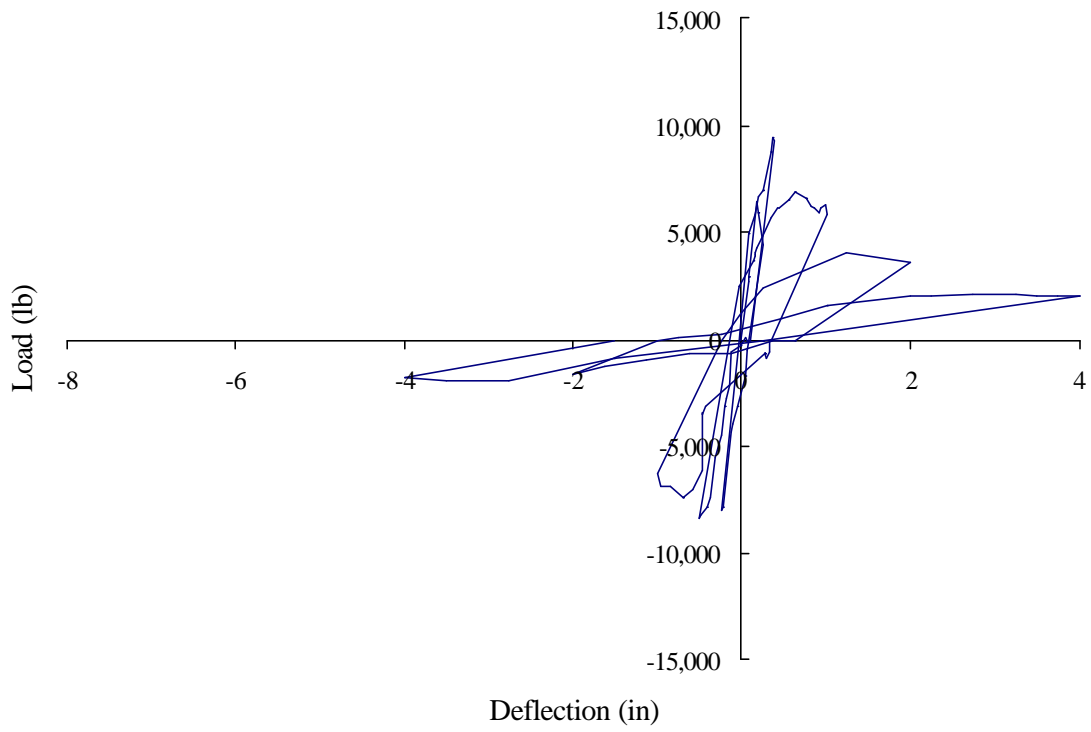


Figure 4.6 Hysteresis loop for plain beam-column joint #6 with 4-in (10.2-cm) spacing

4.2 Strain Plots

The data reported in the following sections includes all that was acquired during testing. Data not reported is due to unforeseen experimental set-up errors (e.g., damaged strain gages).

Cyclical bar strains for SFRC beam-column joint # 1 are shown in Figures 4.7 through 4.9. Bar strains for SFRC joint #5 are shown in Figures 4.10 and 4.11.

Figures 4.12 through 4.15 show bar strains for SFRC joint #2. Bar strains for SFRC joint #4 are shown in Figures 4.17 and 4.18.

Figures 4.18 through 4.20 show bar strains for conventional joint #3. Figures 4.21 through 4.23 show bar strains for conventional joint #6.

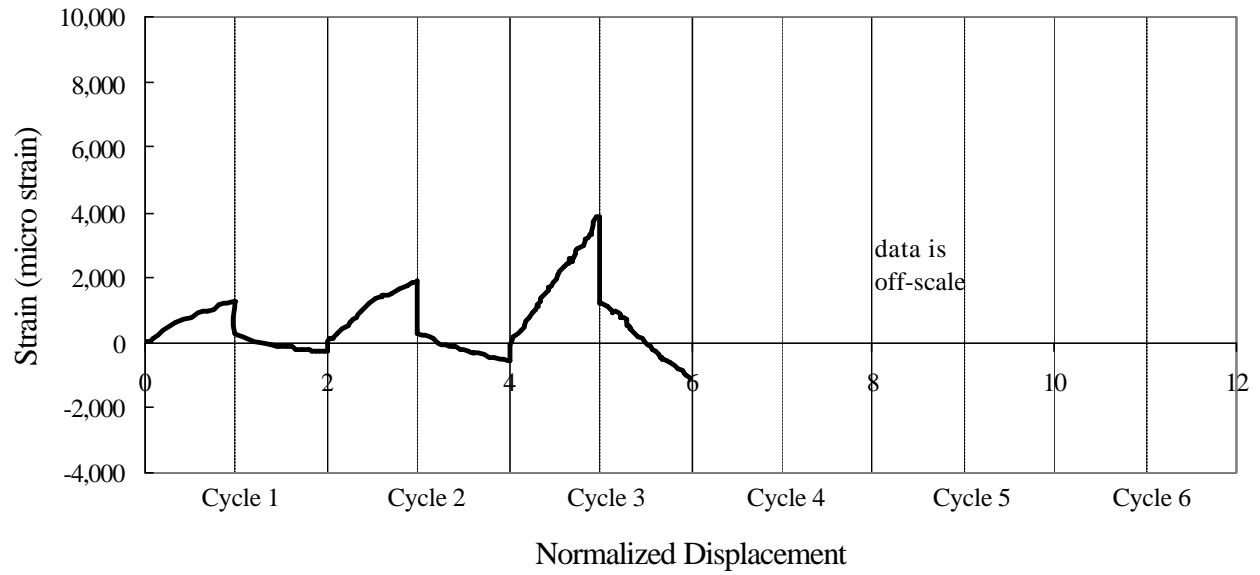


Figure 4.7 BC-Joint # 1 history of strain vs. normalized displacement for #5 bar within beam

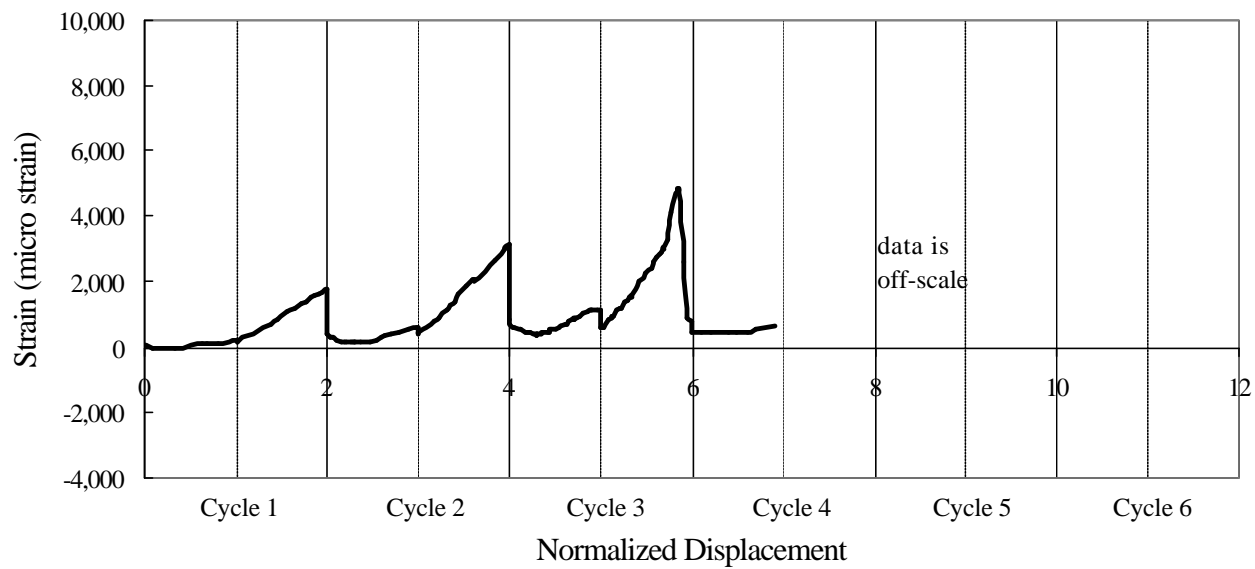


Figure 4.8 BC-Joint #1 history of strain vs. normalized displacement for #4 bar within beam

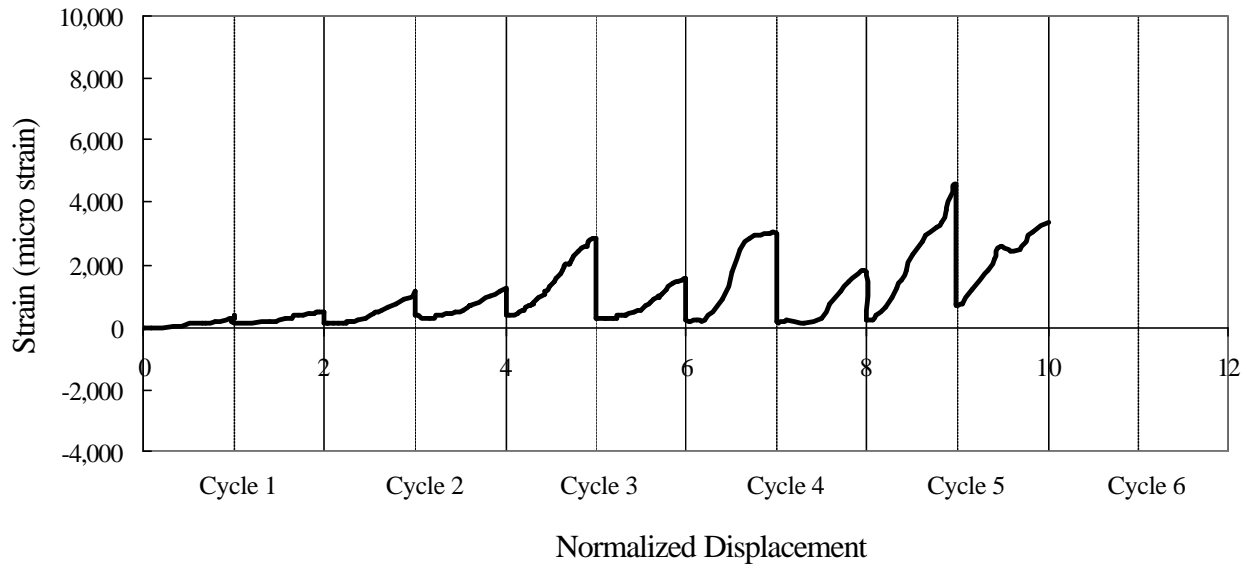


Figure 4.9 BC-Joint #1 history of strain vs. normalized displacement for top column bar

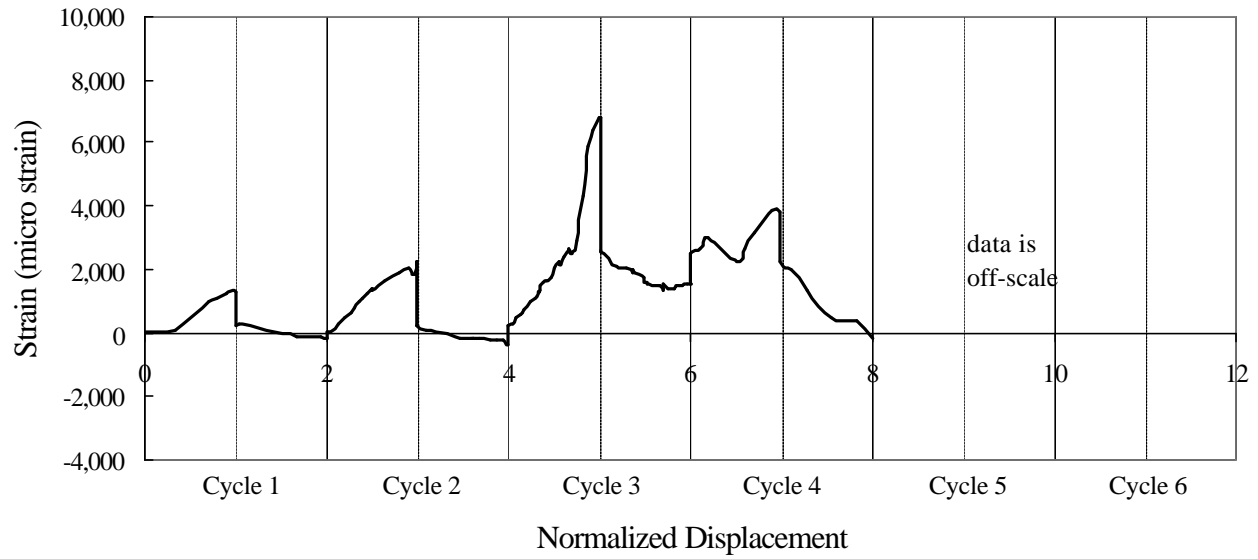


Figure 4.10 BC-Joint #5 history of strain vs. normalized displacement for #5 bar within beam

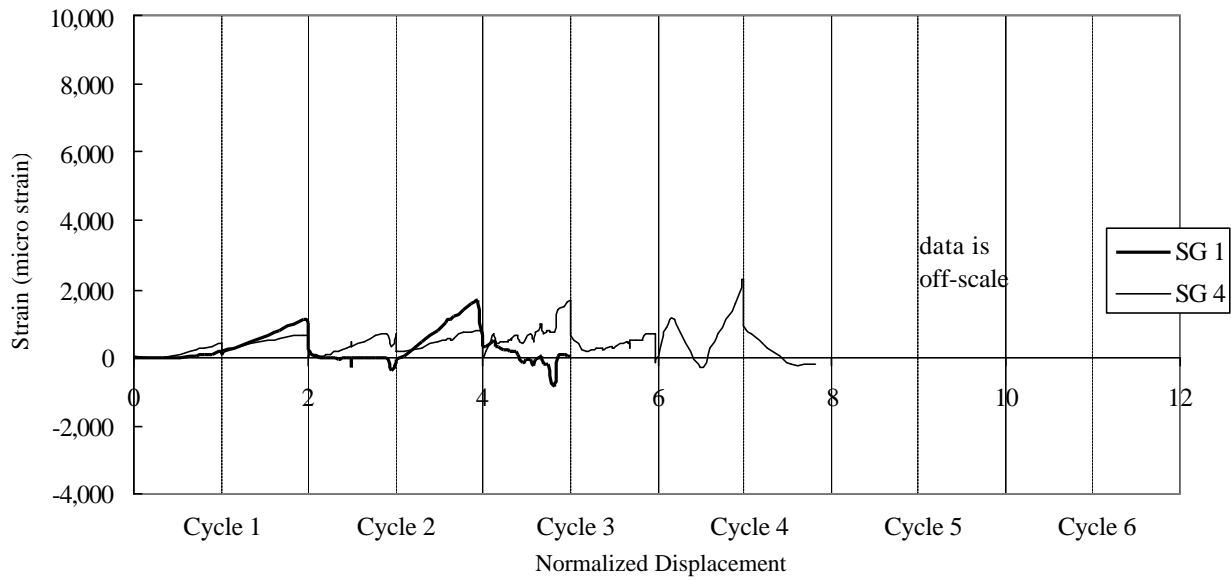


Figure 4.11 BC-Joint #5 history of strain vs. normalized displacement for #4 bar within beam

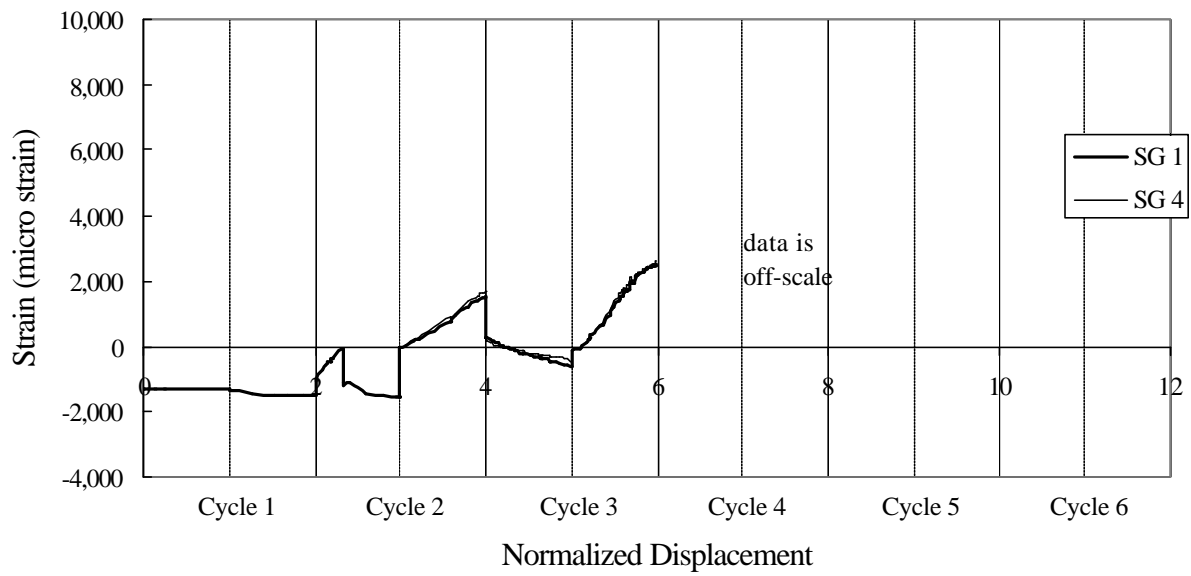


Figure 4.12 BC-Joint #2 history of strain vs. normalized displacement for #5 bar within beam

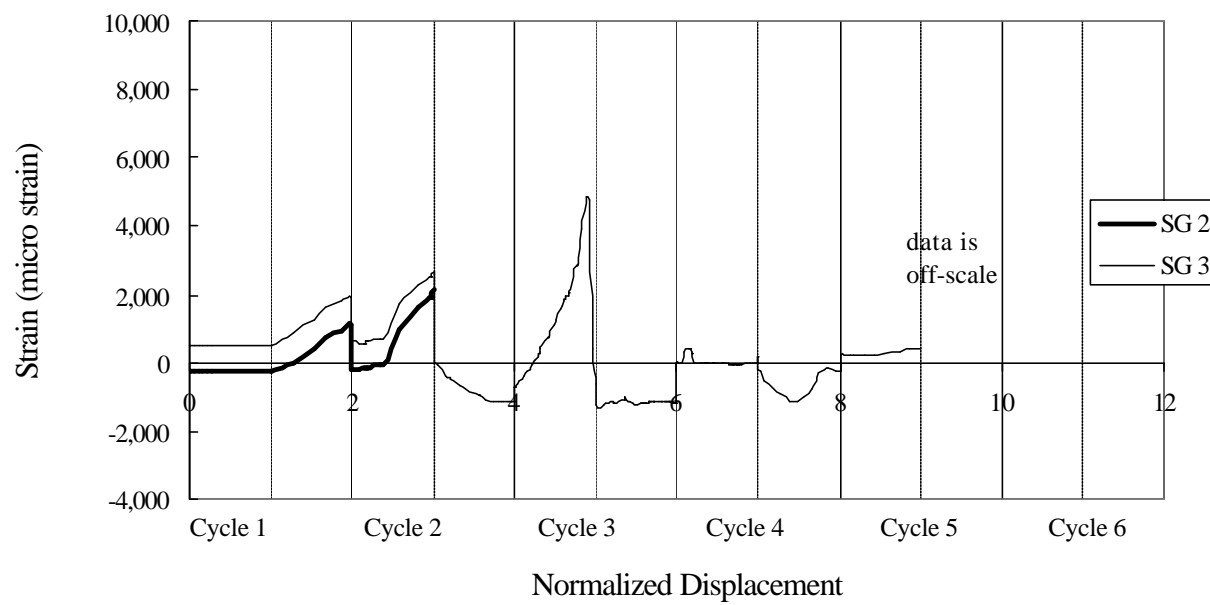


Figure 4.13 BC-Joint #2 history of strain vs. normalized displacement for #4 bar within beam

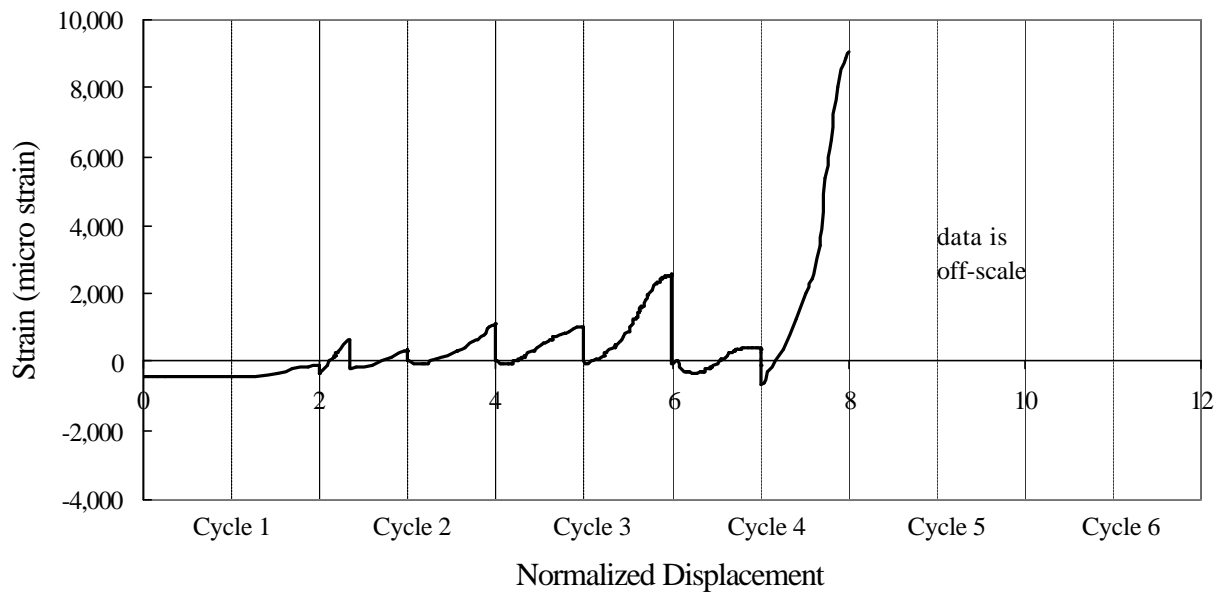


Figure 4.14 BC-Joint #2 history of strain vs. normalized displacement for top column bar

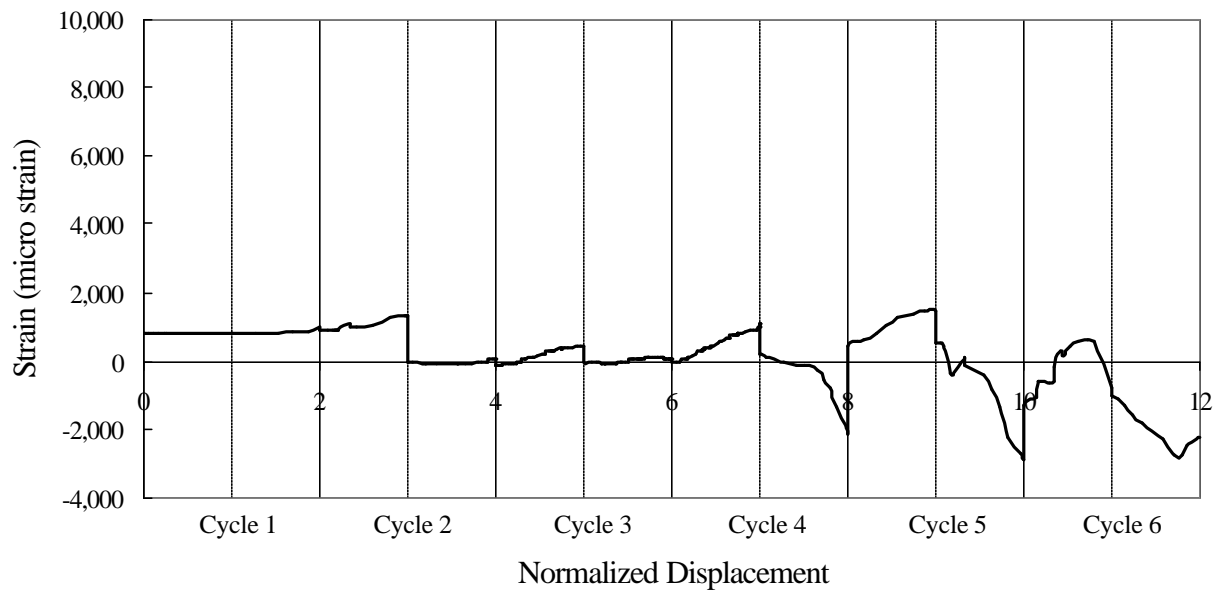


Figure 4.15 BC-Joint #2 history of strain vs. normalized displacement for bottom column bar

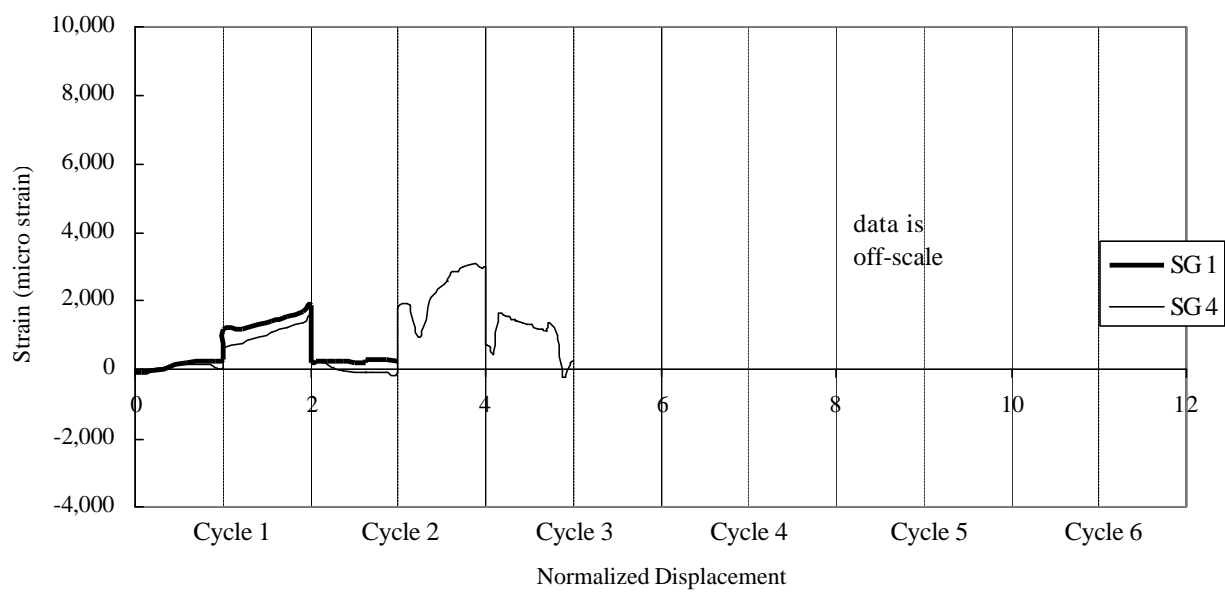


Figure 4.16 BC-Joint #4 history of strain vs. normalized displacement for #4 bar within beam

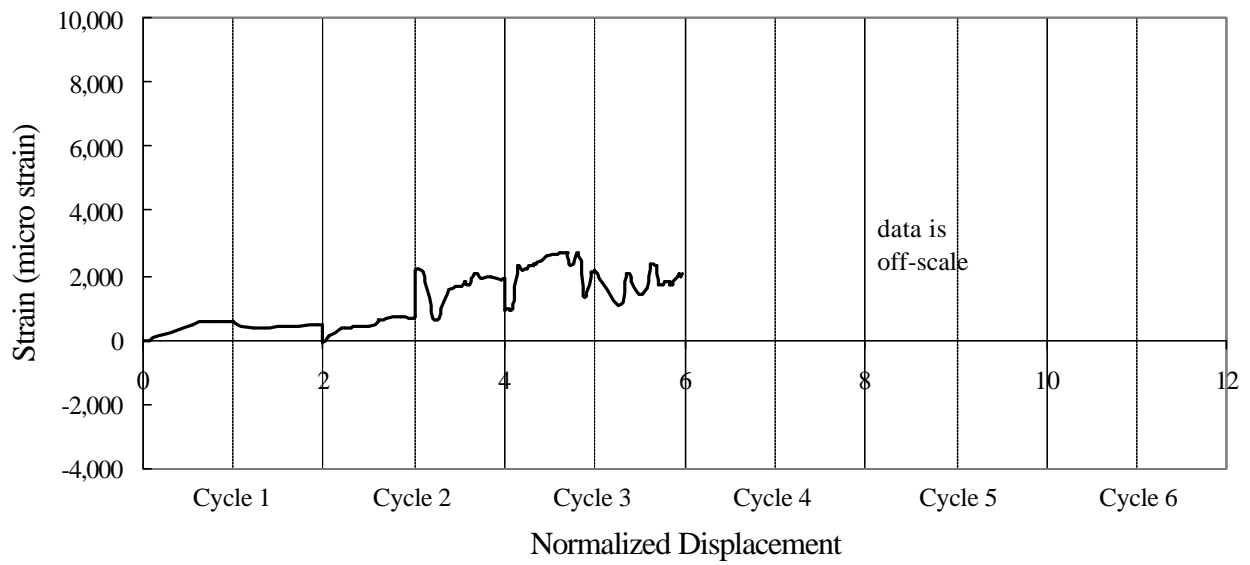


Figure 4.17 BC-Joint #4 history of strain vs. normalized displacement for bottom column bar

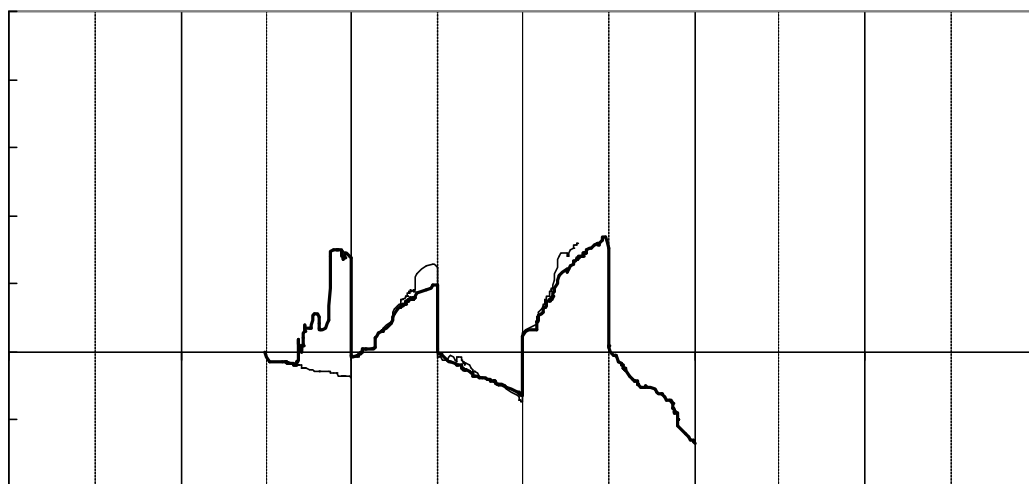


Figure 4.18 BC-Joint #3 history of strain vs. normalized displacement for #5 bar within beam

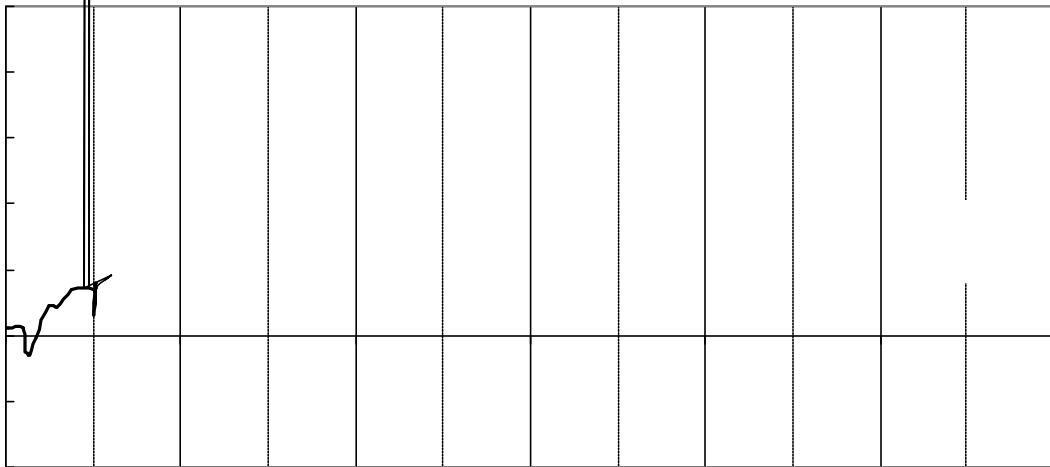


Figure 4.19 BC-Joint #3 history of strain vs. normalized displacement for #4 bar within beam

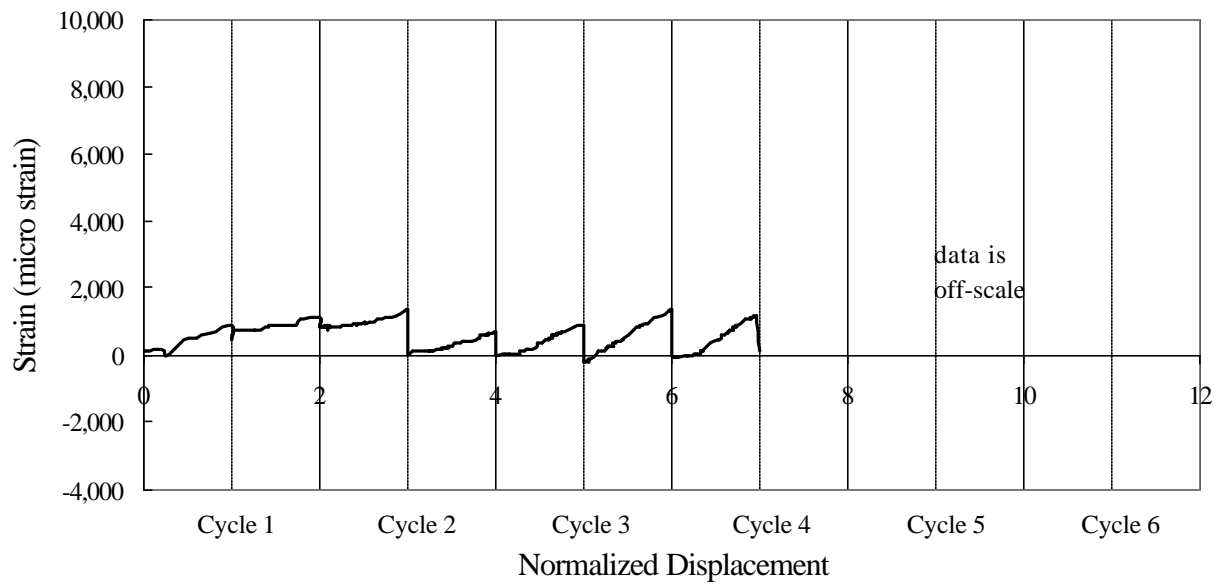


Figure 4.20 BC-Joint #3 history of strain vs. normalized displacement for bottom column bar

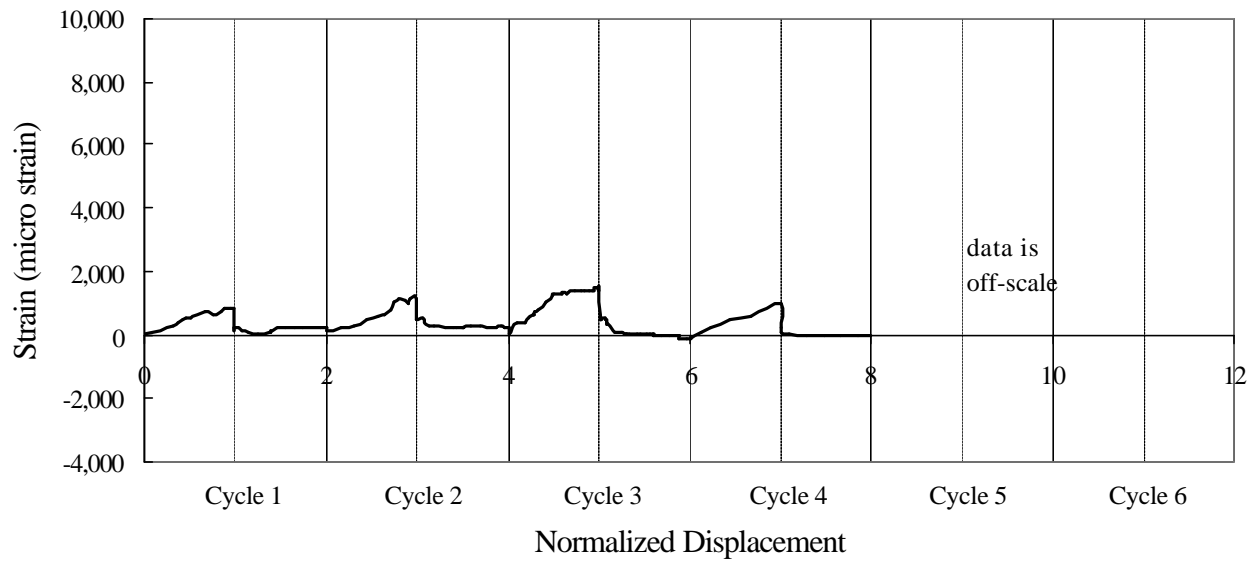


Figure 4.21 BC-Joint #6 history of strain vs. normalized displacement for #5 bar within beam

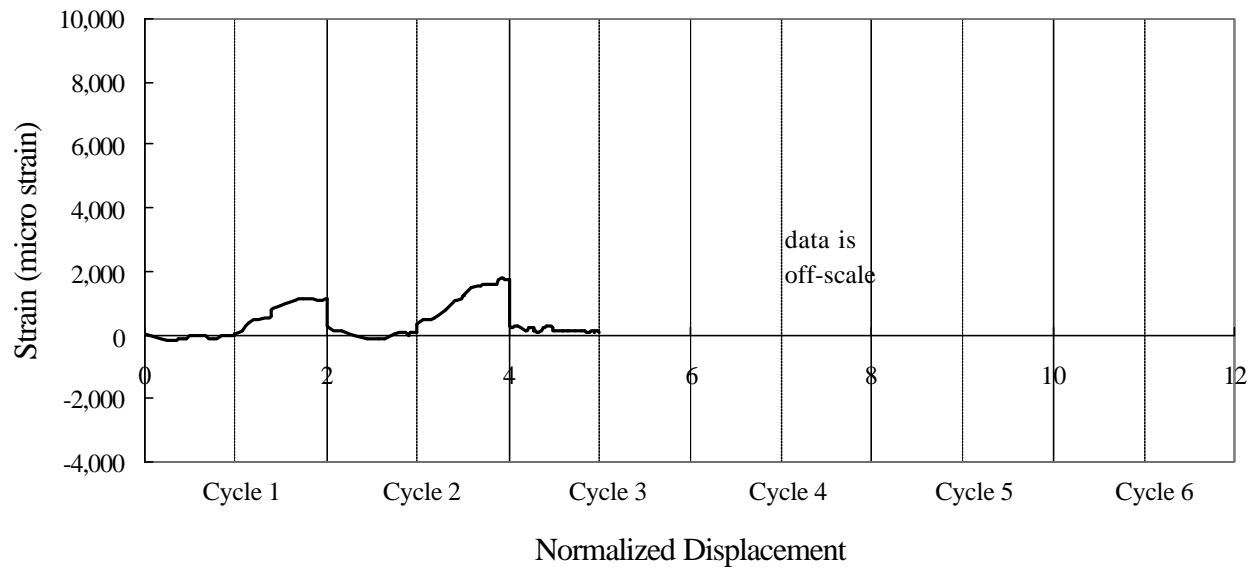


Figure 4.22 BC-Joint #6 history of strain vs. normalized displacement for #4 bar within beam

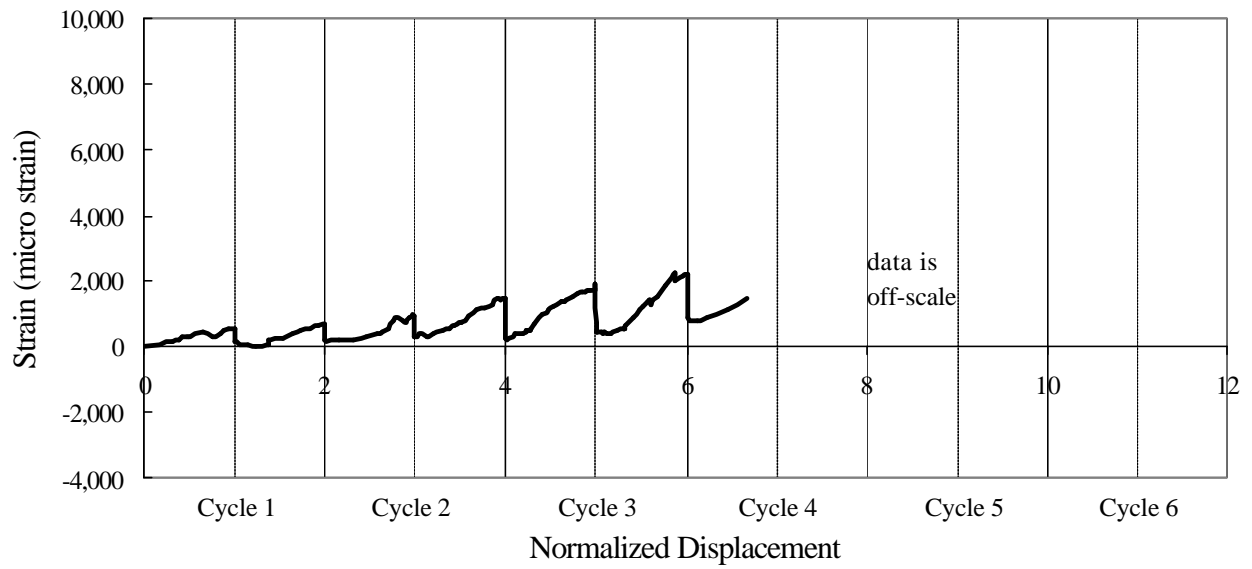


Figure 4.23 BC-Joint #6 history of strain vs. normalized displacement for top column bar

4.3 Quality Testing Results

Results of quality testing were recorded for the compression tests, bar tests, and concrete mix tests.

4.3.1 Compression Tests

Compression tests performed on three plain concrete cylinders resulted in an average compressive strength of 3,460-psi (23.9-MPa). The three SFRC cylinders tested resulted in an average compressive strength of 3,240-psi (22.3-MPa).

4.3.2 Bending Tests

Tensile tests of six beams under third point loading showed that SFRC had a greater tensile strength than plain concrete. The average load at failure for SFRC was 4,500-lb (20-kN) versus 2,817-lb (12.5-kN) for plain concrete. SFRC had an average modulus of rupture of 850-psi (5.8-MPa), whereas the plain concrete specimens produced an average of 520-psi (3.5-MPa).

4.3.3 Other Tests

The concrete mix tests results showed the plain concrete mix had a 6.5-in (16.5-cm) slump (4-in was estimated), 3% air voids, a unit weight of 141.3-lb/ft³ (2,265-kg/m³) and a temperature of 80°F (26.6°C). The room temperature was 76°F (24.4°C). The steel fiber concrete mix, with 2% steel fibers, had a 2-in (5.1-cm) slump, a 20-sec inverted slump cone test time, a temperature of 78°F (25.6°C) and a unit weight of 145.7-lb/ft³ (2,335-kg/m³).

CHAPTER 5

ANALYSIS

This chapter compares hysteresis envelop data, photographs of testing, maximum loads, and strains for the three types of joints tested.

5.1 Hysteresis Loop Envelop

Figure 5.1 illustrates the average envelope of the hysteresis loops of beam-column joints based on the data in Chapter 4. As shown in Figure 5.1, the 6-in (15.2-cm) SFRC joint g, maxim dise pceinntis o1/4 8-in 0.64.3-cmnt

and the conventional joints. Furthermore, the SFRC 8-in (20.3-cm) joints were also superior to the conventional joints in later cycles.

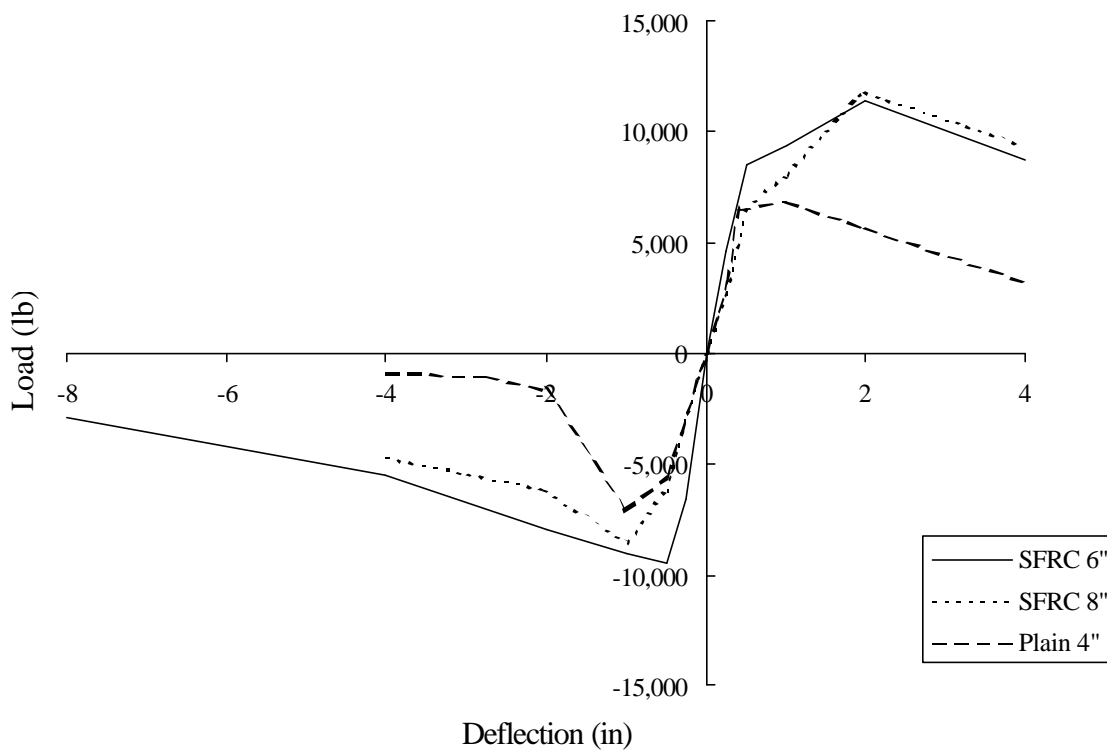


Figure 5.1 Hysteresis envelop curves

Table 5.1 Energy absorbed during the simulated quasi-static earthquake loading

Cycle	Joint											
	SFRC with 6-in (15.2-cm) spacing		SFRC with 8-in (20.3-cm) spacing		SFRC with 8-in (20.3-cm) spacing							
	BC-J 1	BC-J 5	BC-J 2	BC-J 4	BC-J 2	BC-J 4	BC-J 2	BC-J 4	BC-J 2	BC-J 4	BC-J 2	BC-J 4
ft*lb	ft*lb	ft*lb	ft*lb	ft*lb	ft*lb	ft*lb	ft*lb	ft*lb	ft*lb	ft*lb	ft*lb	ft*lb
1 1st half	30 (45)	20 (90)	-	10 (15)	-	10 (15)	-	10 (15)	-	-	-	40 (50)
1 2nd half	40 (50)	10 (40)	-	5 (7)	-	5 (7)	-	5 (7)	-	-	-	40 (50)
2 1st half	120 (160)	170 (760)	90 (120)	50 (70)	-	50 (70)	-	50 (70)	-	-	-	90 (120)
2 2nd half	180 (240)	170 (760)	-	210 (280)	-	210 (280)	-	210 (280)	-	20 (30)	-	60 (80)
3 1st half	410 (530)	330 (1,470)	450 (610)	190 (260)	450 (610)	190 (260)	450 (610)	190 (260)	450 (610)	140 (190)	-	270 (370)
3 2nd half	320 (430)	350 (1,560)	280 (380)	270 (370)	280 (380)	270 (370)	280 (380)	270 (370)	280 (380)	180 (240)	-	210 (280)
4 1st half	570 (780)	1,040 (4,630)	875 (1,190)	350 (470)	875 (1,190)	350 (470)	875 (1,190)	350 (470)	875 (1,190)	350 (470)	-	370 (500)
4 2nd half	600 (820)	650 (2,890)	600 (810)	620 (840)	600 (810)	620 (840)	600 (810)	620 (840)	600 (810)	320 (430)	-	130 (180)
5 1st half	1,780 (2,420)	1,530 (6,810)	1,400 (1,900)	1,500 (2,030)	1,400 (1,900)	1,500 (2,030)	1,400 (1,900)	1,500 (2,030)	1,400 (1,900)	630 (850)	-	280 (380)
5 2nd half	-	1,120 (4,980)	600 (810)	830 (1,130)	600 (810)	830 (1,130)	600 (810)	830 (1,130)	600 (810)	-	-	220 (300)
6 1st half	-	1,180 (5,230)	-	-	-	-	-	-	-	-	-	-
6 2nd half	-	-	-	-	-	-	-	-	-	-	-	-

(-) data not available

5.3 Durability

Typically SFRC resists cracking damage better than plain concrete. The chart of observed damage patterns (Figure 5.2) shows that the SFRC beam-column joints resisted cracking better than the plain concrete beam-column joints. The chart is organized into the 3 categories: beam, column, and joint, so that the cyclical formation of damage in these 3 elements can be compared for the 3 types of test specimens.

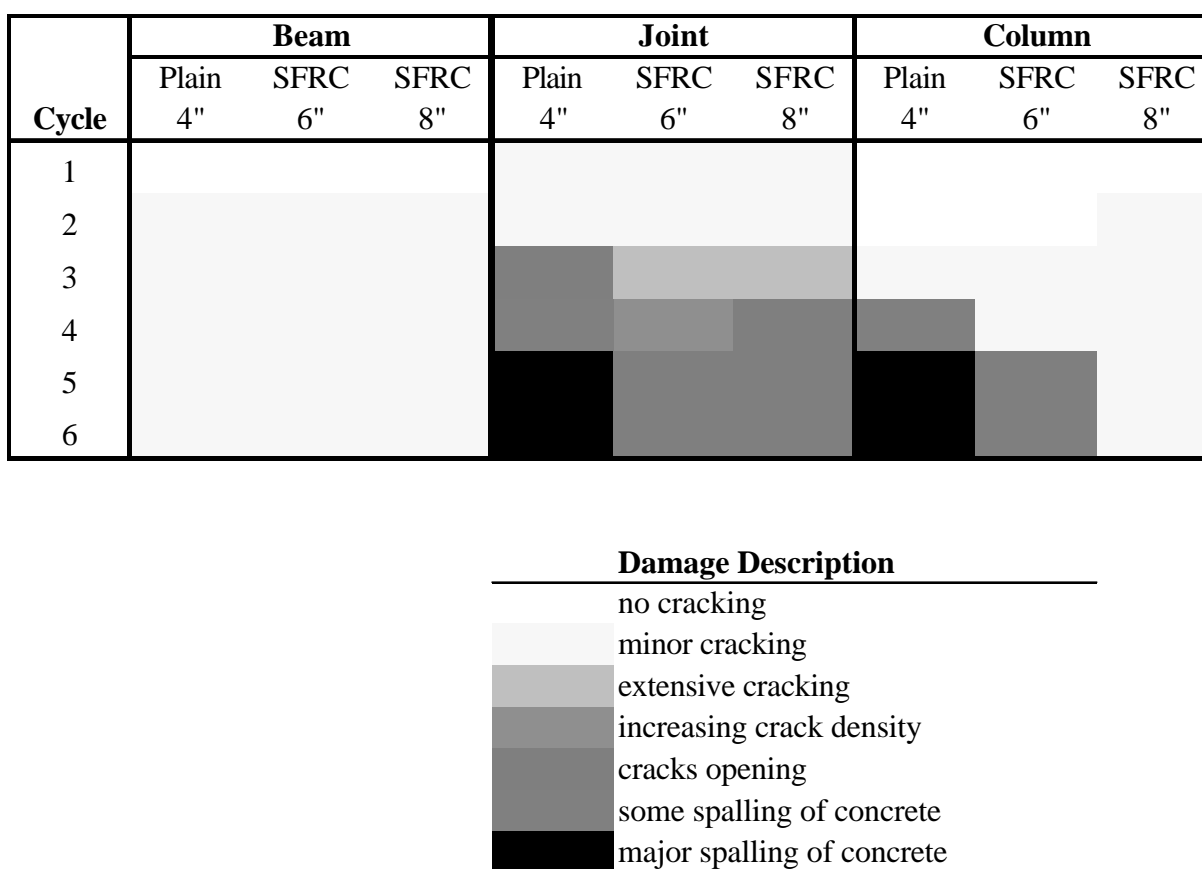


Figure 5.2 Observed damage patterns

5.3.1 Beam Cracking

The beams for all test specimens suffered minor cracking starting at the 2nd cycle and ending with the last cycle of the test.

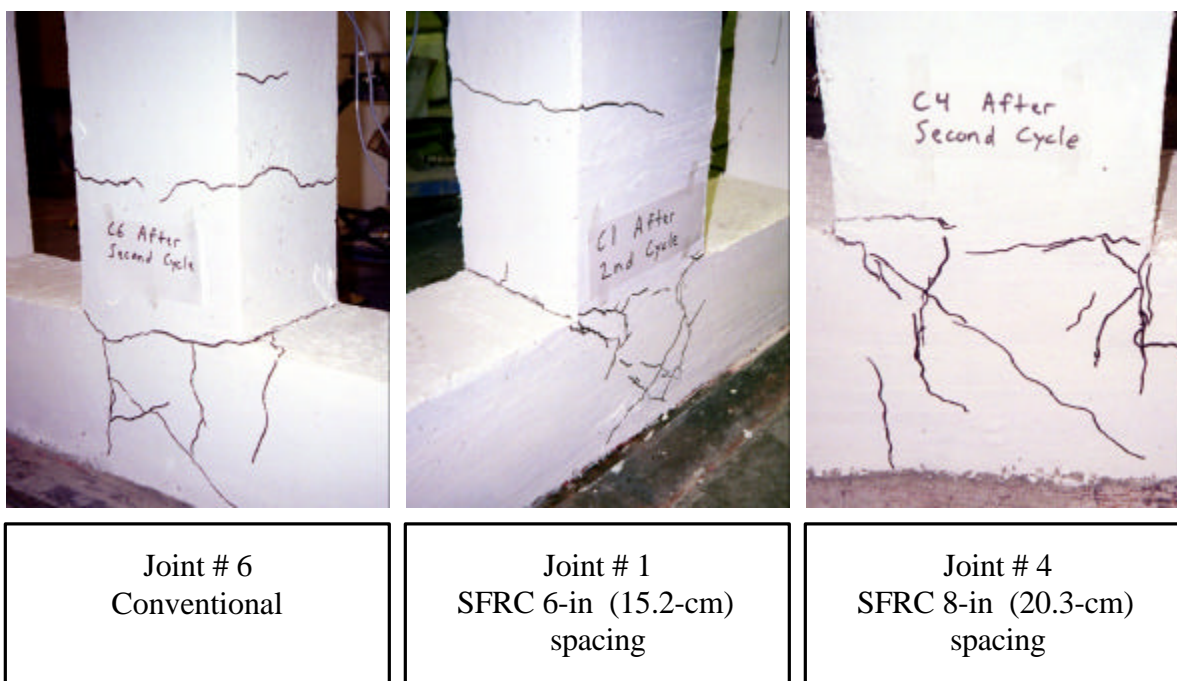
5.3.2 Column Cracking

Visible Cracking in the column was best resisted by the SFRC specimens with 8-in spacing, although the 6-in (15.2-cm) SFRC joint exhibited superior behavior. For SFRC specimens, minor beam cracks began forming during the 2nd cycle and continued to grow until the end of testing. The SFRC specimen with 6-in spacing developed minor beam cracks during the 3rd cycle, however some of those cracks began opening up during the 5th cycle and continued to open up during the 6th cycle. The plain concrete specimens did not fare as well as the SFRC specimens. Minor beam cracks started forming during the 3rd cycle. However, spalling of concrete, began during the 4th cycle. Major spalling of beam concrete occurred during the 5th and 6th cycles.

5.3.3 Joint Cracking

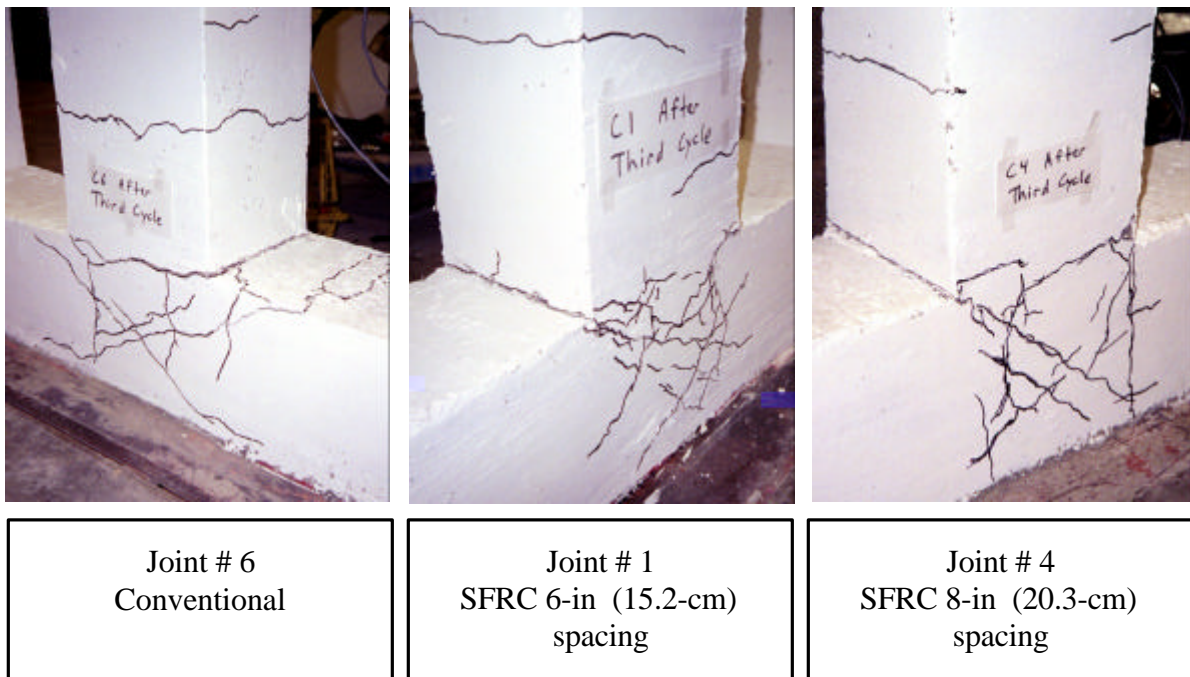
Joint cracking was best resisted by the SFRC specimens with 6-in (15.2-cm) spacing. Minor cracking of the joint began during the 1st cycle. The joint cracks became more extensive during the 3rd cycle and increased in density during the 4th cycle. A crack across the top of the joint opened during the 5th cycle and continued to open up during the 6th cycle. The SFRC specimen with 8-in (20.3-cm) spacing performed almost as well as the SFRC specimen with 6-in (15.2-cm) spacing. Minor cracks began forming during the 1st cycle and became more extensive during the 3rd cycle. A crack across the top of the joint opened during the 4th cycle and continued to open up until the end of testing. The plain concrete specimens exhibited inferior performance. Minor cracks began forming during the 1st cycle. Some of these cracks opened during the 3rd cycle and led to spalling of joint concrete during the 4th cycle. The spalling became more extensive during the 5th and 6th cycles. Figures 5.3 through 5.6 illustrate the above-mentioned discussion.

Spalling and cracking in the SFRC joints was confined by the steel fibers, as shown by Figures 5.3 through 5.6, which allowed for a better bond between steel and concrete to preserve a good portion of its strength. This increased the effectiveness of joint reinforcement.



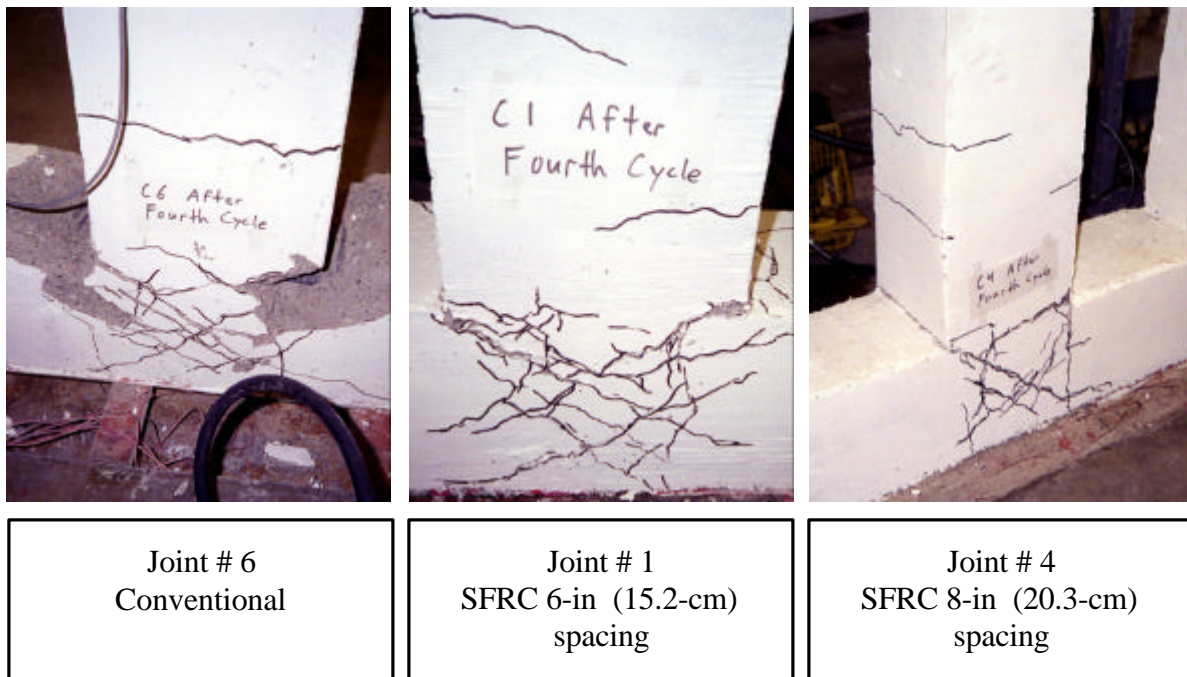
Beam deflection for cycle 2 was 0.5-in (1.3-cm)

Figure 5.3 Observations after cycle 2



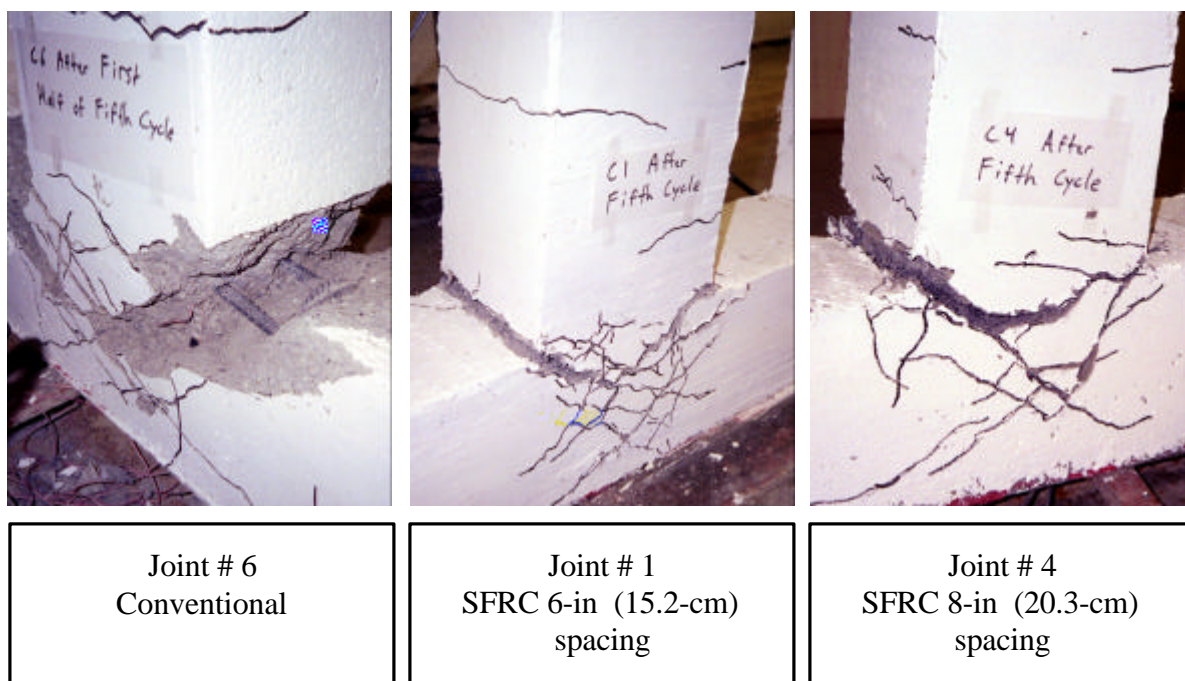
Beam deflection for cycle 3 was 1-in (2.5-cm)

Figure 5.4 Observations after cycle 3



Beam deflection for cycle 4 was 2-in (5.1-cm)

Figure 5.5 Observations after cycle 4



Beam deflection for cycle 5 was 4-in (10.2-cm)

Figure 5.6 Observations after cycle 5

5.4 Seismic Resistance

Based on Figure 5.1, the maximum load for each joint during each cycle is represented in Table 5.2. During the initial cycles, the difference between the maximum loads was minor. However, after cycle 3 the SFRC specimens reached greater maximum loads. By the fifth cycle, the conventional joints exhibited a fraction of the maximum load reached by the SFRC joints.

Table 5.2 Maximum loads reached during the simulated quasi-static earthquake loading

5.5 Strains

Comparisons of strain between SFRC specimens and conventional specimens are shown in Figures 5.7 through 5.12. Each plot shows the strains recorded versus the normalized displacement for the load cycles. Comparisons cannot be made for all cycles due to unforeseen

cm) spacing, and joint #3, conventional, are shown in Figures 5.7 through 5.9. Figure 5.7 shows that during the third cycle, SFRC reached a greater strain for the #5 beam bar. In Figure 5.8, SFRC reached a greater strain during cycles 2 and 3 for the #4 beam bar. After the first half of cycle 2, SFRC reached greater strains for the top column bar.

Figures 5.10 through 5.12 compare strains for joint #2, SFRC with 8-in (20.3-cm), and joint #6, conventional. In Figure 5.10, the #5 beam bar, in the SFRC joint, is in tension during the second half of load cycles whereas the conventional has its beam bar in tension during the first half of the load cycles. This is due to the arrangement of the bars. The figure shows SFRC to reach greater strains during cycles 2 and 3. Figure 5.11 shows SFRC to reach greater strains during cycles 1 and 2. Figure 5.12 shows the column bar strains to be close during the initial cycle. At the conclusion of cycle 3, SFRC reached a greater strain, however, in cycle 4 the strain increased at a greater rate.

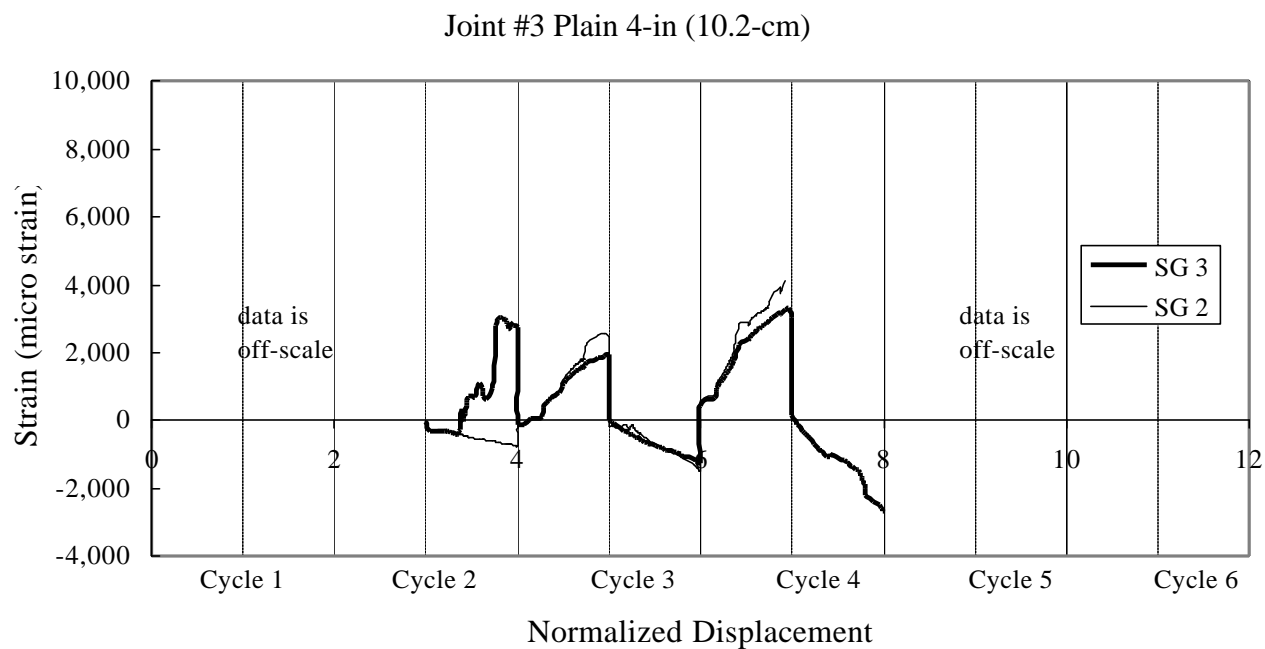
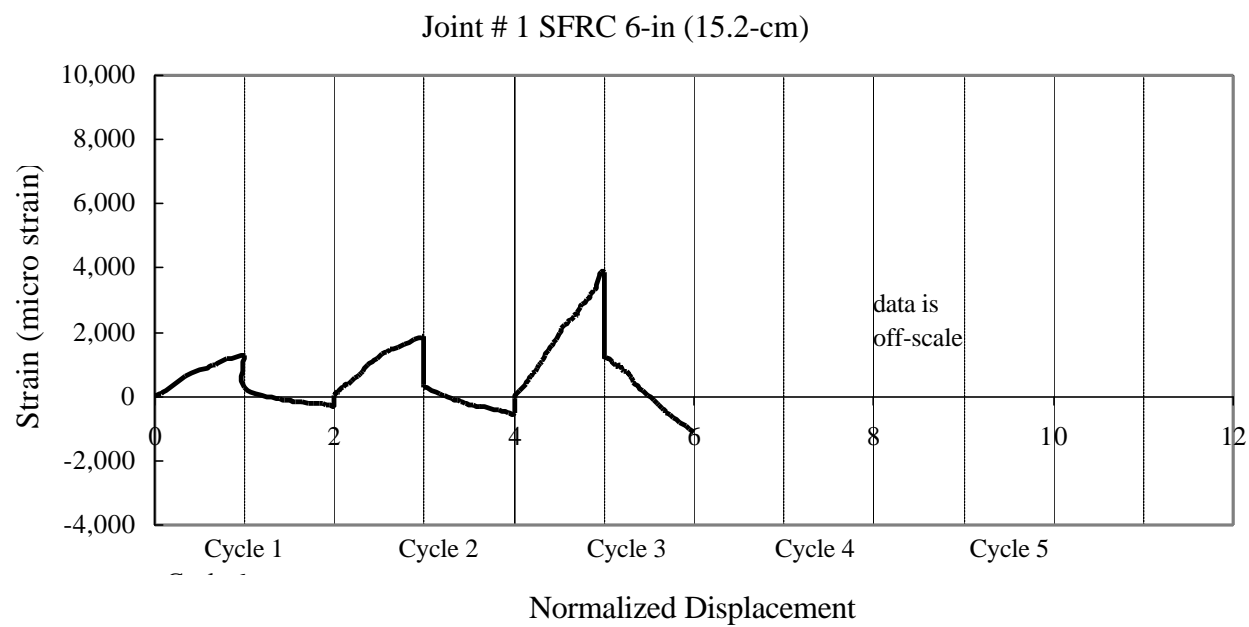


Figure 5.7 Strain comparison between joints 1 and 3 for #5 beam bar

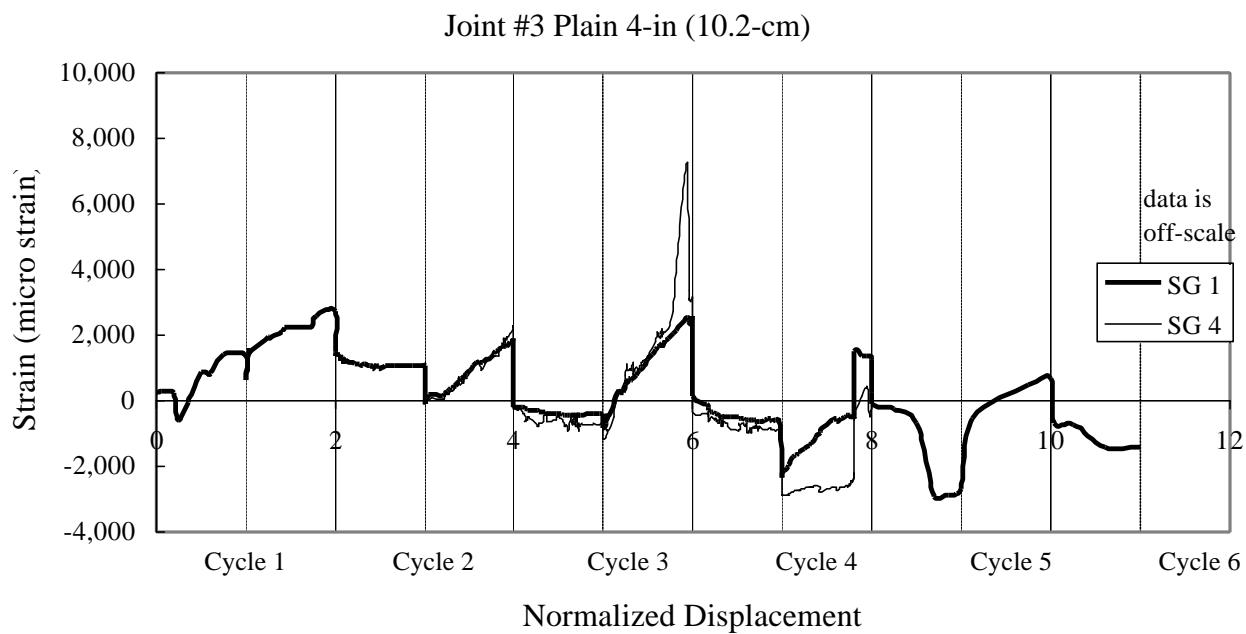
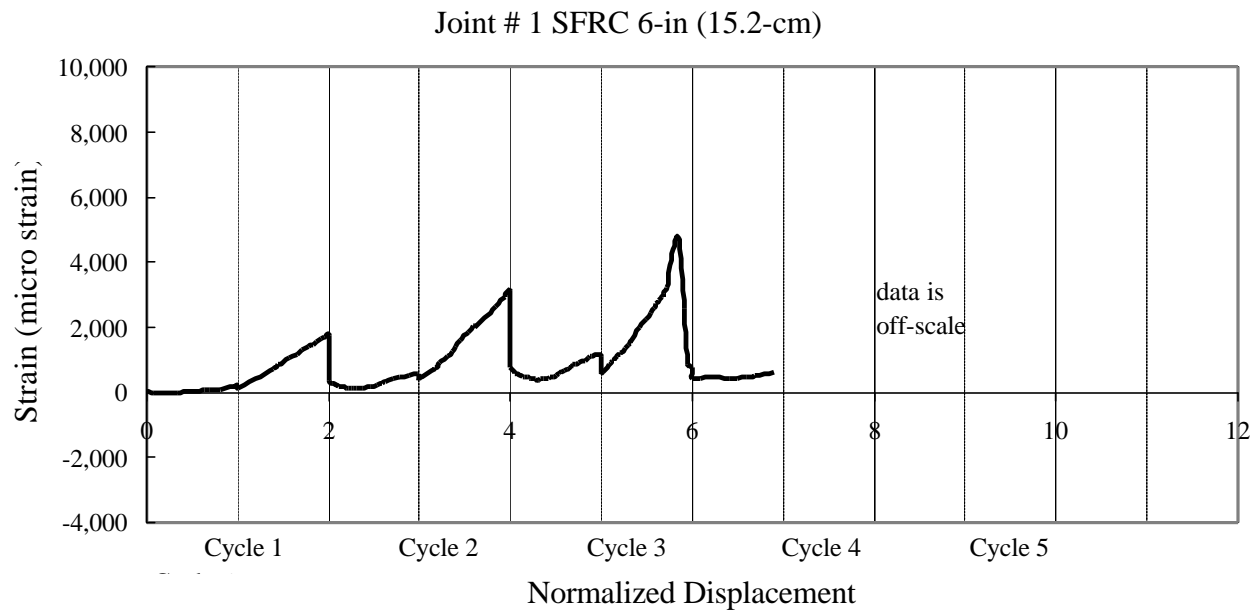


Figure 5.8 Strain comparison between joints 1 and 3 for #4 beam bar

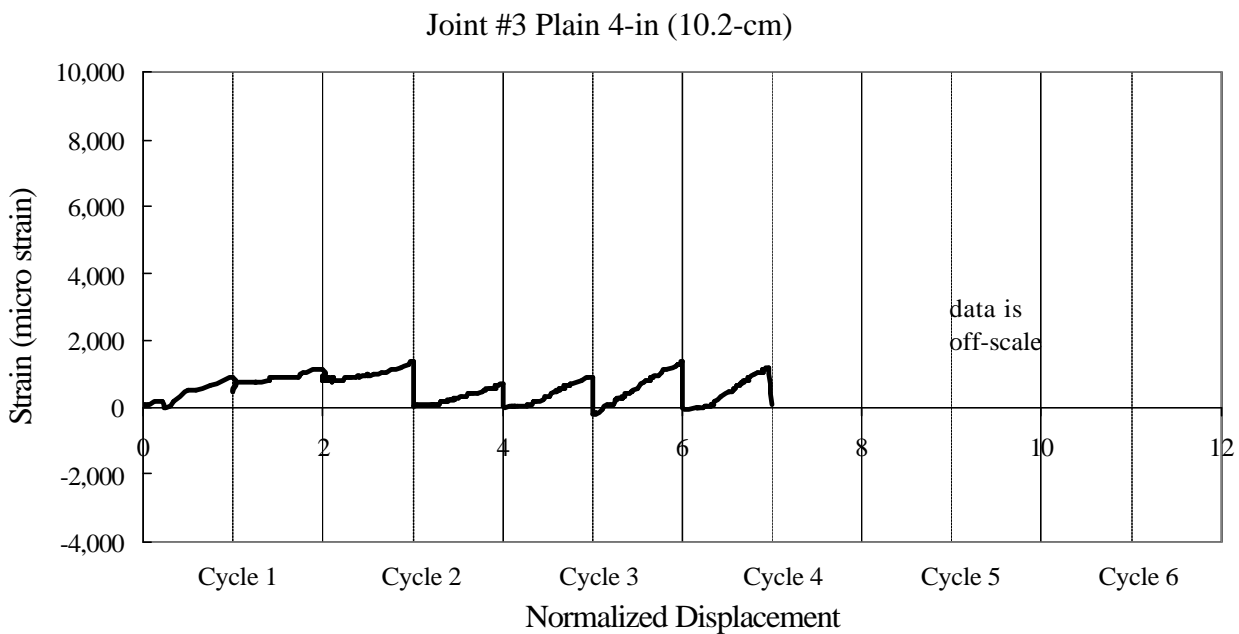
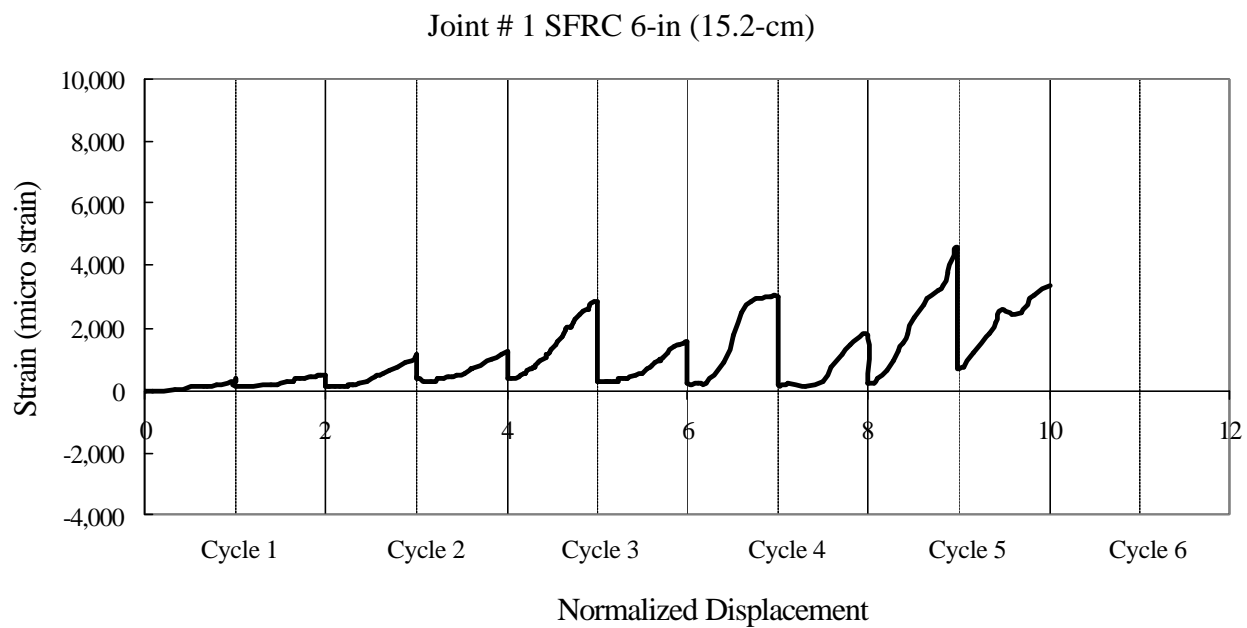


Figure 5.9 Strain comparison between joints 1 and 3 for top column bar

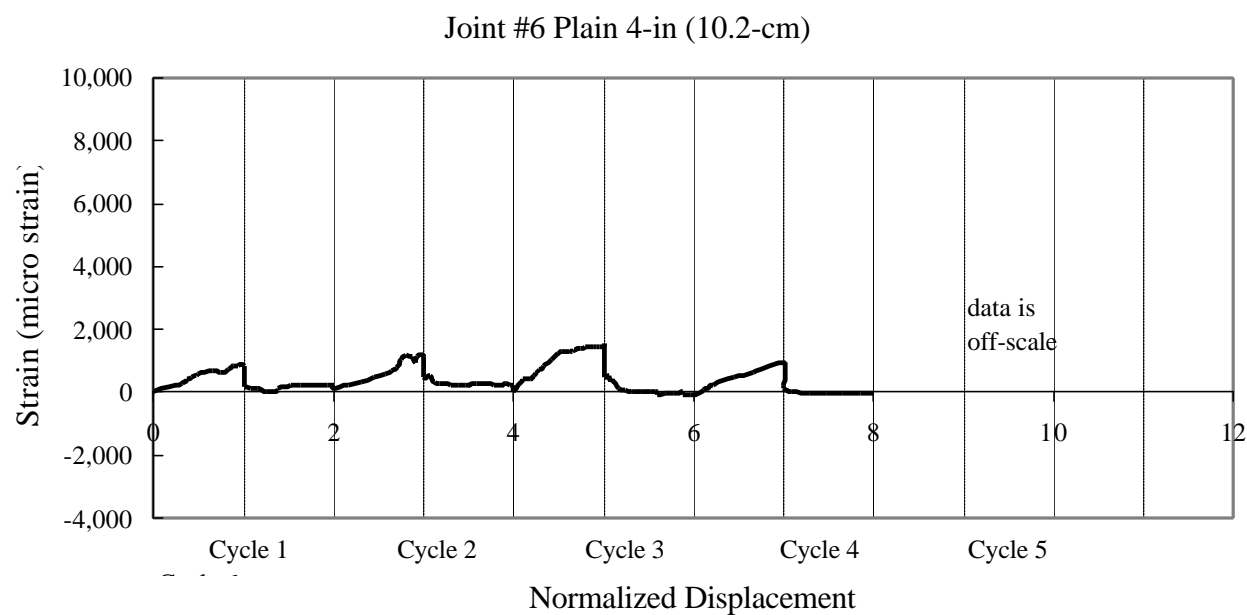
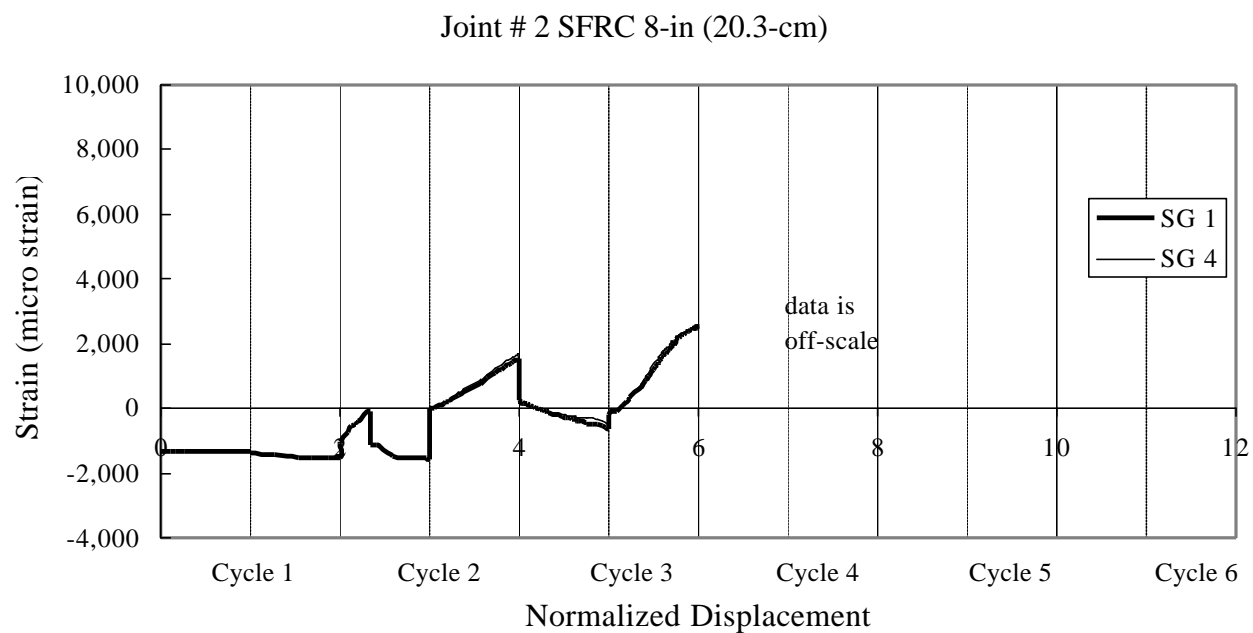
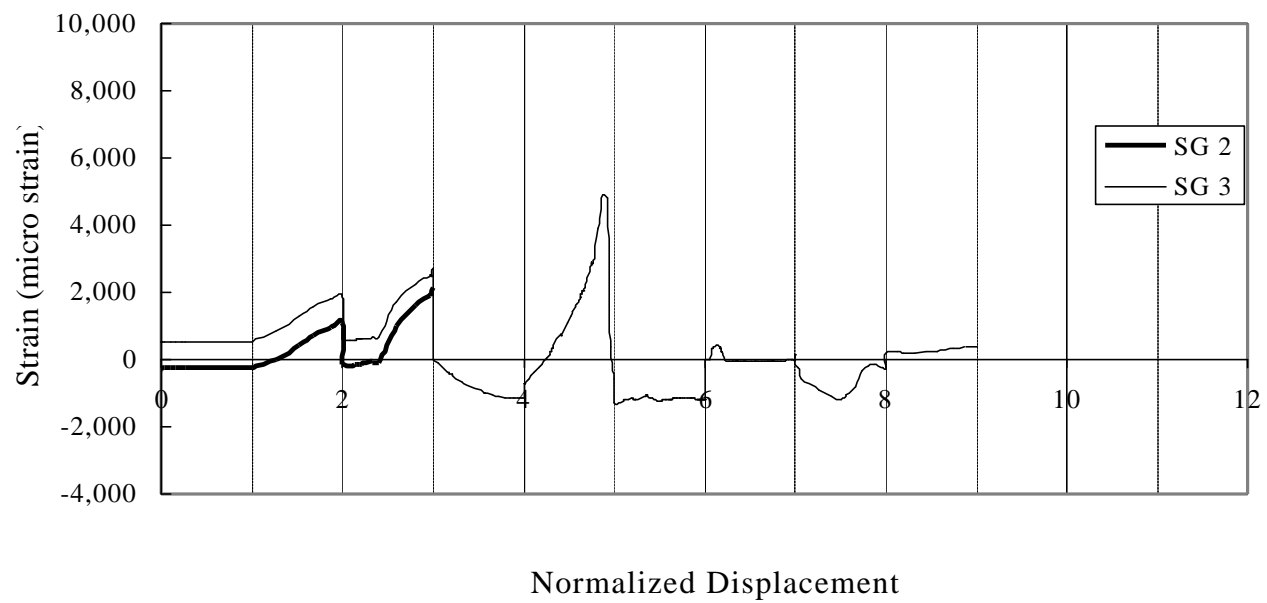


Figure 5.10 Strain comparison between joints 2 and 6 for #5 beam bar



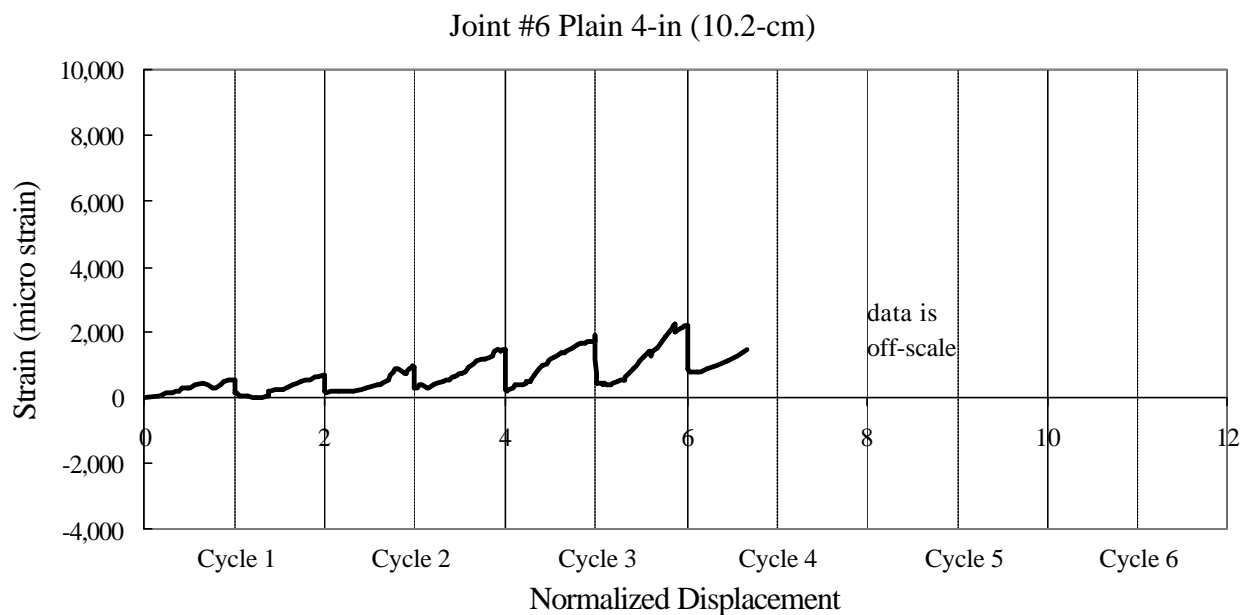
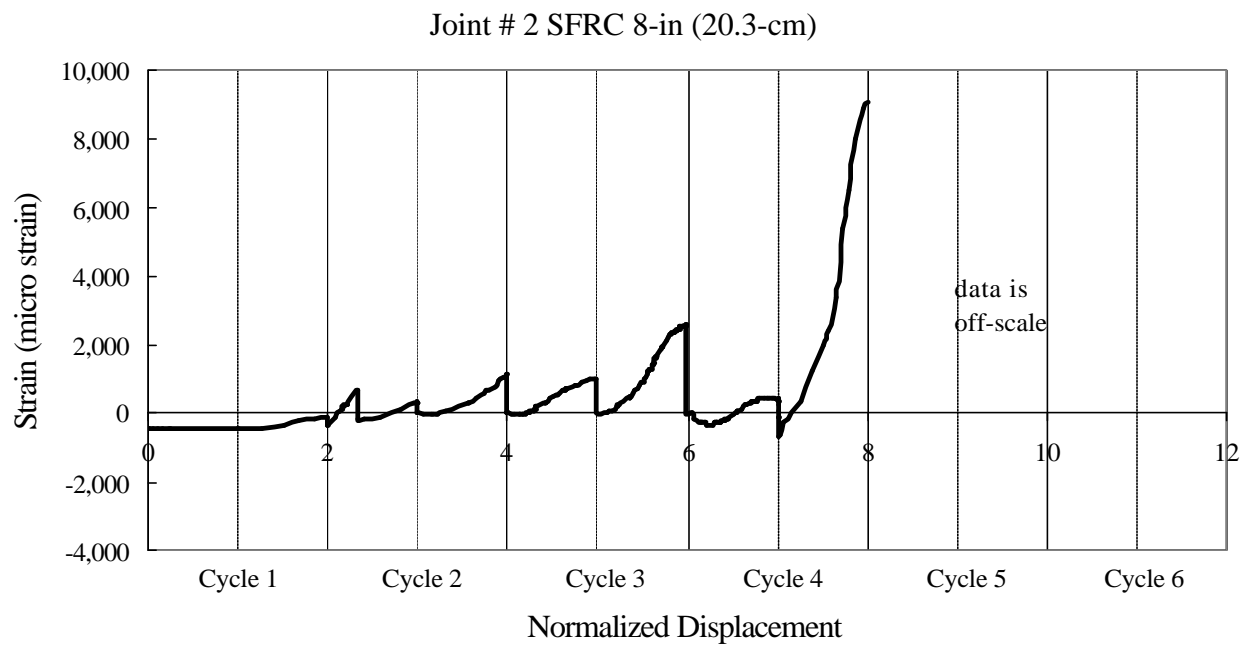


Figure 5.12 Strain comparison between joints 2 and 6 for top column bar

CHAPTER 6

CONCLUSION

Results from this study will be compared to studies conducted by other researchers in this chapter. Also, design recommendations for seismic strength and simplicity of construction will be discussed.

6.1 Comparisons with Previous Studies

Results from this study are comparable to previous research efforts. This study showed that SFRC joints with 6-in (15.2-cm) and 8-in (20.3-cm) spacing had an increase in energy absorption, over the conventional joint, of 173% and 90% respectively. Other researchers have come across similar findings in their studies, and are discussed in greater detail in Chapter 2.

Henager was the first to experiment with SFRC joints and observe the increase in ductility. He was able to conclude that SFRC could replace joint hoops [7]. Frame testing conducted by Lakhshmipathy and Santhahumar showed increases of 57% for ductility and a 130% for cumulative energy dissipation [8]. Gefken and Ramey found SFRC joints to have better energy dissipation ductility and concluded that joint hoop spacing could be increased

Although similarities can be drawn between this study and others, this study pioneers all efforts in bar strains by showing that steel bars are more effective in fiber joints. Evidence in section 5.5 showed the SFRC specimens to have greater bar strains throughout cycle 2. Soubra, Wight and Naaman measured joint bar strains in pre-cast SFRC joint specimens [12]. However, the joints constructed lacked columns, and were tested under third point loading. They concluded that testing of connections that are more realistic was needed because third point loading subjected the joint to a constant moment and to no shear force. Jiuru, in 1992, also used strain gages on beam bars of a joint [19]. From the strain data, they were able to calculate an average bond stress of 1,030-psi (7.1-MPa) for SFRC joints versus 770-psi (5.3-MPa) for plain joints. However, no conclusions were made of the bar strain.

6.2 Seismic Strength

The joints with 6-in (15.2-cm) spacing had by far a better seismic resistance than the SFRC joint with 8-in (20.3-cm) which itself had an improved seismic resistance over the plain concrete joint with 4-in (10.2-cm) spacing. This is seen by the hysteresis loops, hysteresis envelop curve and by observations made of the testing. These exterior SFRC joints would prevent structural collapse of a building unlike the code designed plain concrete joint.

6.3 Simplification of Construction

The SFRC joints with 8-in (20.3-cm) spacing exhibited greater seismic strength than the plain concrete joint with 4-in (10.2-cm) spacing, as seen by the hysteresis loops, hysteresis envelope curve and by observations of testing. This SFRC joint could be advantageous in an area at low risk of very high seismic motion. It would be advantageous

because it could reduce difficulty encountered when placing hoops in beam-column joints. Hoop spacing can be increased by a factor of 2 thus providing a more simplified beam-column joint construction technique.

6.4 Design Recommendations

It is recommended that for exterior beam-column joints, in which ease of construction is desired, steel fibers at a volume fraction of 2% can be used with code hoop spacing increased by a factor of 2. For exterior joints in high seismic risk areas, an SFRC joint with the same volume fraction and a code hoop spacing increased by a factor of 1.5 (at a maximum) can be used. If the hoop spacing is increased by a factor less than 1.5, it is likely that an even stronger seismic joint can be produced.

REFERENCES

1. MacGregor, J. *Reinforced Concrete Mechanics and Design*. 3rd ed. New Jersey: Prentice Hall, 1997.
2. Johnston, C. "Fiber Reinforced Concrete." *Significance of Tests and Properties of Concrete and Concrete-Making Material*, ASTM STP 169C, 1994, pp. 547-561.
3. Bayasi, Z. "Development and Mechanical Characterization of Carbon Fiber Reinforced Cement Composites & Mechanical Properties and Structural Applications of Steel Fiber Reinforced Concrete." Dissertation for the Degree of Ph.D., Michigan State University, 1989, V.1, pp. 1-199.
4. Bayasi, Z., R. Bhattacharya, and M. Posey. "Fiber Reinforced Concrete: Basics and Advancements," *Proceedings, Symposium on Advancements in Concrete Materials*, Bradley University, 1989, pp. 1-1 to 1-27.
5. Bayasi, Z., and H. Kaiser. "Steel Fibers as Crack Arrestors in Concrete." *The Indian Concrete Journal*, to be published April 2001.
6. Soroushian, P., and Z. Bayasi. "Local Bond Behavior of Deformed Bars in Steel Fiber Reinforced Concrete Joints." *Magazine of Concrete Research*, June 1990, pp. 39-43.
7. Henager, C.H. "Steel Fibrous, Ductile Concrete Joint for Seismic Resistant Structures." *Reinforced Concrete Structures in Seismic Zones*, SP 53-14, American Concrete Institute, Detroit, 1977, pp. 371-386.
8. Lakshmipathy, M., and A. Santhakumar. "Experimental Verification of the Behaviour of Reinforced Fibrous Concrete Frames Subjected to Seismic Type of Loading." *Third International Symposium on Developments in Fibre Reinforced Cement and Concrete*, Rilem, July 1986.
9. Jindal, R., and V. Sharma. "Behavior of Steel Fiber Reinforced Concrete Knee-Type Beam-Column Connections." *Fiber Reinforced Properties and Applications*, SP-105, American Concrete Institute, Detroit, 1987, pp. 475-491.
10. Olariu, I., A. Ioani, and N. Poenar. "Steel Fiber Reinforced Ductile Joints," *Ninth World Conference on Earthquake Engineering*, Tokyo-Kyoto, Japan, Aug.1988, pp. 657-662.
11. Gefken, P.R., and M.R. Ramey. "Increased Joint Hoop Spacing in Type 2 Seismic Joints Using Fiber Reinforced Concrete." *ACI Structural Journal*, Mar-Apr. 1989, pp. 168-172.

12. Soubra, K., J. Wight, and A. Naaman. "Fiber Reinforced Concrete Joints for Precast Construction in Seismic Areas." *ACI Structural Journal*, Mar-Apr. 1991, pp. 214-221.
13. Olariu, I., A. Ioani, and N. Poienar. "Seismic Behaviour of Steel Fiber Concrete Beam-Column." *Tenth World Conference on Earthquake Engineering*, Madrid, Spain, July 1992, pp. 3169-3174.
14. Sood, V., and S. Gupta. "Behavior of Steel Fibrous Concrete Beam-Column Connections." *Fiber Reinforced Concrete and Applications*, SP-105, American Concrete Institute, Detroit, 1987, pp. 437-474.
15. Craig, R., J. McConnell, H. Germann, N. Dib, and F. Kashani. "Behavior of Reinforced Fibrous Concrete Columns." *Fiber Reinforced Concrete International Symposium*, SP-81, American Concrete Institute, Detroit, 1984, pp. 69-105.
16. Jindal, R., and K. Hassan. "Behavior of Steel Fiber Reinforced Concrete Beam-Column Connections." *Fiber Reinforced International Symposium*, SP-81, American Concrete Institute, Detroit, 1982, pp. 107-123.
17. Fattuhi, N. "SFRC Corbel Tests." *ACI Structural Journal*, Mar-Apr. 1987, pp. 119-123.
18. Narayanan R., and I. Darwish. "Use of Steel Fibers as Shear Reinforcement." *ACI Structural Journal*, May-June 1987, pp. 216-227.
19. Jiuru, T., H. Chaobin, Y. Kaijian, and Y. Yongcheng. "Seismic Behavior and Shear Strength of Framed Joint Using Steel-Fiber Reinforced Concrete." *Journal of Structural Engineering*, ASCE, Feb. 1992, pp. 341-358.
20. Filiatrault, A., K. Ladicani, and B. Massicotte. "Seismic Performance of Code-Designed Fiber Reinforced Concrete Joints." *ACI Structural Journal*, Sep-Oct. 1994, pp. 564-571.
21. Filiatrault, A., S. Pineau, and J. Houde. "Seismic Behavior of Steel-Fiber Reinforced Concrete Interior Beam-Column Joints." *ACI Structural Journal*, Sep-Oct. 1995, pp. 543-552.
22. Soroushian, P., and Z. Bayasi. "Strength and Ductility of Steel Fibre Reinforced Concrete Under Bearing Pressure." *Magazine of Concrete Research*, Dec. 1991, pp. 243-248.
23. Craig, R., S. Mahadev, C.C. Patel, M. Viteri, and C. Kertesz. "Behavior of Joints Using Reinforced Fibrous Concrete." *Fiber Reinforced Concrete International Symposium*, SP-81, American Concrete Institute, Detroit, 1984, pp. 125-167.

24. ACI Committee 544 "Guide For Specifying, Mixing, Placing, and Finishing Steel Fiber Reinforced Concrete." American Concrete Institute, 1984.

APPENDIX A**STRAIN DATA FOR BEAM-COLUMN JOINTS**

APPENDIX B**LOAD CELL STRAIN DATA FOR BEAM-COLUMN****JOINTS**

APPENDIX C**BEAM-COLUMN JOINT STRAIN DATA PLOTS**

APPENDIX D

LOAD CELL STRAIN PLOTS

APPENDIX E

PHOTOGRAPHIC TESTING HISTORY

APPENDIX F

1997 UNIFORM BUILDING CODE PERTAINING TO BEAM-COLUMN

JOINT DESIGN

ABSTRACT

ABSTRACT

The research program for this thesis studies the benefits of using steel fiber reinforced concrete in seismic-resistant beam-column joints. By using SFRC in a beam-column joint, some of the difficulties associated with joint construction can be overcome and a greater seismic strength can be provided. Two half-scale joints were constructed to reflect current building code, two SFRC joints were constructed with a hoop spacing increased by 50%, and two SFRC joints were constructed with a hoop increased by 100%. Hooked-end steel fibers with a length of 1.2-in (31-mm), a diameter of 0.020-in (0.50-mm) and an aspect ratio of 60 were used at a volume fraction of 2%. After simulating a quasi-static earthquake loading, the SFRC joints were found to have dissipated more energy than the conventional joints. A 90% increase in energy absorption was found for SFRC joints with hoop spacing increased by 100%. A 173% increase in energy absorption was found for SFRC joints with hoop spacing increased by 50%. It was also found that joint bar reinforcement became more effective in the SFRC joints because of increased bar strains recorded during the simulated quasi-static earthquake loading.